

Petrogenetic evolution of Cretaceous Samchampi-Samteran Alkaline Complex, Mikir Hills, Northeastern India: Implications on multiple melting events of heterogeneous plume and metasomatized sub-continental lithospheric mantle

Abhishek Saha^{1*}, Sohini Ganguly², Jyotisankar Ray³, Christian Koeberl^{4,5}, Martin Thöni⁴, C. Sarbajna⁶ and S.S. Sawant⁷

¹*National Institute of Oceanography (Council of Scientific and Industrial Research)
Dona Paula, Goa- 403 002, India*

²*Department of Earth Science, Goa University Taleigao Plateau, Goa 403206, India*

³*Department of Geology, University of Calcutta, 35, Ballygunge Circular Road, Kolkata 700 019, India*

⁴*Department of Lithospheric Research, University of Vienna, Althanstrasse 14, A-1090 Vienna, Austria*

⁵*Natural History Museum, Burggring 7, A-1010 Vienna, Austria*

⁶*Atomic Minerals Directorate (AMD) for Exploration & Research, Begumpet, Hyderabad 500 016, India*

⁷*National Geophysical Research Institute (Council of Scientific and Industrial Research)
Uppal Road, Hyderabad 500 007, India*

*E-mail: asaha.geocal@gmail.com

Abstract

The Samchampi (26° 13' N: 93° 18'E)-Samteran (26° 11'N: 93° 25'E) alkaline complex (SSAC) occurs as an intrusion within Precambrian basement gneisses in the Karbi-Anglong district of Assam, Northeastern India. This intrusive complex comprises a wide spectrum of lithologies including syenite, ijolite-melteigite, alkali pyroxenite, alkali gabbro, nepheline syenite and carbonatite (nepheline syenites and carbonatites are later intrusives). In this paper, we present new major, trace, REE and Sr-Nd isotope data for different lithologies of SSAC and discuss integrated petrological and whole rock geochemical observations with Sr-Nd isotope systematics to understand the petrogenetic evolution of the complex. Pronounced LILE and LREE enrichment of the alkaline-carbonatite rocks together with steep LREE/HREE profile and flat HREE-chondrite normalized patterns provide evidence for parent magma generation from low degree partial melting of a metasomatized garnet peridotite mantle source. LILE, HFSE and LREE enrichments of the alkaline-silicate rocks and carbonatites are in agreement with the involvement of a mantle plume in their genesis. Nb-Th-La systematics within incompatible trace element abundance patterns marked by positive Nb-Ta anomalies and negative K, Th and Sr anomalies suggest contribution from plume-derived OIB-type mantle with recycled subduction component and a rift-controlled, intraplate tectonic setting for alkaline-carbonatite magmatism giving rise to the SSAC. This observation is corroborated by enriched $^{87}\text{Sr}/^{86}\text{Sr}_{\text{initial}}$ (0.705562 to 0.709416) and $^{143}\text{Nd}/^{144}\text{Nd}_{\text{initial}}$ (0.512187 to 0.512449) ratios for the alkaline-carbonatite rocks that attest to a plume-related enriched mantle (~EM II) source in relation to the origin of Samchampi-Samteran alkaline complex. Trace element chemistry and variations in isotopic data invoke periodic melting of an isotopically heterogeneous, metasomatized mantle and generation of isotopically distinct melt batches that were parental to the different rocks of SSAC. Various extents of plume-lithosphere interaction also accounts for the trace element and isotopic variations of SSAC. The $\text{Sr}_{\text{initial}}$ and $\text{Nd}_{\text{initial}}$ (105 Ma) isotopic compositions (corresponding to ϵ_{Nd} values of -6.37 to -1.27) of SSAC are consistent with those of Sung Valley, Jasra, Rajmahal tholeiites (Group II), Sylhet Traps and Kerguelen plateau basalts.

Keywords: alkaline rocks; carbonatite; enriched mantle; metasomatism; Sylhet Traps

Introduction

Alkaline igneous complexes comprise a wide compositional lithospectrum including ultramafic, mafic, felsic and carbonatite lithologies, which in turn have attracted worldwide academic interest because of their intricate mineralogical compositions, extreme petrographic variability with distinctive geochemical and isotopic signatures (Le Bas, 1987, 1989; Gittins, 1989; Bailey, 1993; Bell et al., 1998; Ray, 2009). Ultramafic-mafic-alkaline-carbonatite magmatism is characterized by high abundances of alkali metals and alkaline earth elements with pronounced enrichments of high field strength elements (HFSE), large ion lithophile elements (LILE), light rare earth elements (LREE) and high volatile contents (Subrahmanyam and Leelanandam, 1989; Veksler et al., 1998; Verhulst et al., 2000; Downes et al., 2005; Doroozi et al., 2015; Poletti et al., 2016). These distinct geochemical attributes provide significant clues to understand the source characteristics, mantle melting conditions, tectonic setting and petrogenetic evolution of alkaline-carbonatite complexes (Le Bas, 1987; Nelson et al., 1988; Deines, 1989; Wyllie et al., 1990; Bell and Blenkinsop, 1989; Simonetti and Bell, 1994; Srivastava and Taylor, 1996; Bell et al., 1998; Harner, 1999; Bell and Simonetti, 1996, 2010; Ma et al., 2011).

Ultramafic-mafic-alkaline-carbonatite associations, including their plutonic and volcanic varieties, originate from partial melts of asthenospheric mantle and represent differentiation centres of continental (CFB) and oceanic (OFB) flood basalt provinces collectively reflecting plume magmatism in rift-controlled, intraplate tectonic regime (Heaman et al., 2002; Doroozi et al., 2015). These alkaline-carbonatite complexes mark the initiation and cessation periods of the main flood basalt event and occur as intrusive equivalents of flood basalt magmas (Hart et al., 1992; Basu et al., 1993; Toyoda et al., 1994; Franz et al., 1999; Bell, 2001; Ghatak and Basu, 2011; 2013). The generation of flood basalts and associated alkaline-carbonatite magmas has been attributed to the melting of a volatile-rich plume head (Sen, 1995; Ray et al., 2000). The alkaline-carbonatite complexes occurring in association with plume-hotspot related flood basalt volcanism provide valuable information on the chemical evolution of mantle reservoirs, distinct modes of mantle melting and interaction between mantle plume and sub-continental lithospheric mantle (SCLM; Lassiter and DePaolo, 1997; Marzoli et al., 2000; Grange et al., 2010).

In eastern and northeastern India, the eruption of Rajmahal-Sylhet flood basalts (~117 Ma; Baksi, 1995) is believed to record the first manifestation of Kerguelen plume activity on the Indian plate in the c. 120-100 Ma time window (Mahoney et al., 1983; Storey et al., 1992; Class et al., 1993; Ray and Pande, 2001; Ray et al., 2005). The Shillong Plateau and the Mikir Hills of northeastern India host ultramafic-mafic-alkaline-carbonatite complexes (Fig. 1), which represent

various phases of the Sylhet Trap magmatism, a part of Rajmahal-Sylhet flood basalts (Ray et al., 1999; Srivastava and Sinha, 2004a; 2004b; Srivastava et al., 2005; Ghatak and Basu, 2011; 2013). The present study focuses on Samchampi (26°13' N: 93°18' E) - Samteran (26°11' N: 93°25' E) alkaline complex (SSAC; Fig. 2), which is one of those centres related to Sylhet Traps, and it occurs as a near circular intrusive body emplaced within the Precambrian gneissic terrane in the Mikir Hills of northeastern India. This paper reports new major and trace (including REE) element and Sr-Nd isotopic data for the alkaline-mafic-ultramafic rocks and carbonatites of SSAC, northeastern India. The petrological and geochemical data (including Sr-Nd isotope systematics) of SSAC have been utilized to address (i) the petrogenetic processes involved in the generation of alkaline-silicate rocks and carbonatites; (ii) the mantle source enrichment processes; (iii) the role of mantle metasomatism in producing alkaline-carbonatite magmas; (iv) mantle melting conditions; (v) the influence of plume-lithospheric interaction on alkaline-carbonatite magmatism in rift-related intracontinental tectonic environment; and (vi) geochemical and isotopic correlations of SSAC with Sylhet Traps and Kerguelen plume.

2. Geological Setting

The Shillong Plateau forms part of the northeastern extremity of the Indian peninsular shield. It is an oblong-shaped, northward tilting, uplifted horst-like feature covering an area of about 40,000 km². The Shillong Plateau is bound in the north and south by the E-W trending Brahmaputra fault systems and the north-dipping Dauki fault, respectively (Fig. 1). The western and eastern fringes of the plateau are bordered by the Jamuna fault and the N-W striking Kopili fault, respectively- the latter separating the Shillong Plateau from the Mikir Hills (Fig. 1; Evans, 1964; Desikachar, 1974; Nandy, 1980, 2001; Acharyya et al., 1986; Gupta and Sen, 1988; Nakata, 1989; Biswas and Grasemann, 2005; Srivastava and Sinha, 2007; Kayal et al., 2006; Yin et al., 2010). The Mikir Hills comprise the eastern extension of the Shillong Plateau and extend over an area of about 7000 km² (Hussain and Ahmad, 2009; Majumdar, 2010). The Archaean basement gneissic complex of the Shillong Plateau and Mikir Hills consists of two different units viz. gneissic complex proper and the non-porphyrific migmatitic granitoids (Mazumder 1986; Nandy, 2001). The Shillong Group metasediments, consisting of phyllite, mudstone, sandstone and coarse-grained, cross-bedded quartz arenite, were deposited in a 240 km long, NE-SW trending intracratonic basin resting unconformably over the basement gneissic complex and are metamorphosed to greenschist facies (Nandy, 2001). The Proterozoic mafic magmatic rocks of the Shillong Plateau occur as concordant and discordant intrusions within the Shillong Group of rocks. Neoproterozoic porphyritic granites occur as discordant plutons cutting across the Shillong Group of metasediments and

basement gneisses (Ray et al, 2013). The Cretaceous Sylhet Trap basalts represent the next stratigraphic unit in the Shillong Plateau and Mikir Hills, which are believed to be the result of Kerguelen plume activities (Baksi, 1995; Ray et al., 1999). The Sylhet Trap basalts are associated with alkaline-carbonatite complexes intruding the Precambrian gneisses and Shillong Group metasediments. These intrusive complexes occur in Sung Valley (Srivastava and Sinha, 2004a; 2004b; Srivastava et al., 2005; Melluso et al., 2010), Swangkre-Rongmill (Srivastava and Sinha, 2007; Srivastava et al., 2016), Jasra (Srivastava and Sinha, 2007; Melluso et al., 2012), Samchampi-Samteran (Saha et al., 2010a; 2010b; 2011), and Mawpyut (Chaudhuri et al., 2014). NE-SW and ENE-WSW trending linear fracture patterns subparallel to the Kalyani Lineament and the Sarhed fault (Nandy, 1980; 2001; Nag et al., 1999), are interpreted as pathways for the emplacement of alkaline-carbonatite complexes and seismic activity. The youngest lithological unit of the Shillong Plateau and Mikir Hills is represented by Tertiary shelf sediments occupying the southern fringe of the plateau.

The SSAC was emplaced into the Precambrian granite gneisses of the Mikir Hills in the Karbi-Anglong district of Assam (Fig.2). This intrusive complex comprises a wide variety of lithologies, including syenite, ijolite-melteigite, alkali pyroxenite, alkali gabbro, nepheline syenite and carbonatite. Syenite constitutes the dominant lithology of the complex and the ijolite-melteigite suite of rocks occurs as intrusion within the syenite giving an arcuate outcrop pattern (Fig. 2). Alkali pyroxenite and alkali gabbro occur as inliers within the ijolite-melteigite suite. Vanadium-bearing titaniferous magnetite ore bodies are exposed as isolated intrusives within the syenite host rocks (Fig.2) (Saha et al., 2010a; 2010b). Dykes and dykelets of nepheline syenite and carbonatite occur as later intrusives cutting across the syenite and ijolite-melteigite rocks (Saha et al., 2010a; 2010b).

3. Sampling and Analytical Techniques

Samples were collected from unweathered outcrops and sixty-five thin sections were prepared for optical microscopy. Quantitative modal analyses were performed for thirty-six representative samples (n=36) of the SSAC (Table 1), using the point counting method of Chayes (1949). After petrographic screening, twenty-six (26) samples were selected for major and trace element analyses and six (6) samples for determination of Sr-Nd isotopic ratios. Samples of around 1 kg were crushed, and powdered to a definite size (~120 mesh) using an agate mortar to avoid contamination or loss of homogeneity at all stages.

3.1 Major, trace and rare earth elements

Major oxide compositions were determined using X-ray fluorescence (XRF) at the Atomic Minerals Division (AMD) Laboratory, Hyderabad, India. Pressed powder pellets of the samples were used for the determination of ten major and minor element oxides by XRF. Boric acid powder, used as the binding material, was placed in a collapsible aluminium crucible, over which ~1 g of the homogenized sample powder was sprayed evenly by hand and pressed to form disc shaped pellets (32mm × 3mm) using Herzog Hydraulic press subjected to a variable load pressure of 55-65 kilo-Newton (kN). Loss on Ignition (LOI) was determined by heating powdered samples at 900°C for 4 hours. Philips MagiXPRO PW2400, microprocessor controlled, sequential XRF with a single goniometer-based measuring channel covering the complete elemental range was used for the analyses of major and minor element oxides of representative rock samples from SSAC. The Philips Super Q software was used for matrix corrections. Accuracy and precision are better than 5% RSD (% relative standard deviation). XRF analyses of the six samples selected for Sr-Nd isotope analyses were carried out at the Department of Lithospheric Research, University of Vienna, Austria; standards used in both labs and % RSD are comparable.

Trace element compositions of representative whole rock samples were determined using Inductively Coupled Plasma-Mass Spectrometer (ICP-MS; Perkin Elmer ELAN DRC-II) at the National Geophysical Research Institute (NGRI), Hyderabad, India. All rock samples were analyzed for a total of 28 elements. A mixture of doubly distilled acids (HF: HNO₃:HClO₄) mixed in the ratio 7:3:1 was used for sample digestion. 5ml of 1ppm ¹⁰³Rh (internal standard) was added to each sample for standardization. The details regarding the instrumental parameters are given in Balaram (1992) and Balaram and Gnaneshwar Rao (2003). Certified reference materials SY-2 (for alkaline-felsic and alkaline-mafic rocks) and JP-1 (for alkaline-ultramafic rocks) (Govindaraju, 1994) were used in order to validate the results obtained here and the precision was better than 5% RSD (% Relative Standard Deviation) for all elements. The precision and accuracy based on replicate analyses of international rock standards are 2-5% (1s) for most elements. Trace element concentrations of the six samples selected for Sr-Nd isotope analyses were determined by Instrumental Neutron Activation Analysis (INAA) at the Department of Lithospheric Research, University of Vienna, Austria. The relative precisions of elemental concentrations were mainly 2-20 %. The best relative precisions (less than 10%) were found for the elemental contents of Sc, Cr, Co, Zn, Rb, Zr, Cs, La, Ce, Eu, Tb, Hf and Ta. Measurements were done following procedures described by Koeberl (1993), Son and Koeberl (2005) and Mader and Koeberl (2009). Details of instrumentation, standards, data reduction, accuracy, and precision are given in Mader and Koeberl

(2009). Certified reference materials GSR-3, SY-2 and JP-1 were also analyzed along with the Samchampi-Samteran samples in order to assess the accuracy of the data.

3.2 Sr-Nd isotopes

Sr and Nd isotopic studies were conducted using thermal ionization mass spectrometry (TIMS) at the Laboratory of Geochronology, Department of Lithospheric Research, University of Vienna. Powders of selected representative samples of SSAC were digested in tight Savillex beakers using an ultra pure mixture of HF: HClO₄ (5:1) for 2 weeks at 105°C on a hot plate. After acid evaporation, repeated treatment of the residue using 5.8 N HCl resulted in clear solutions. Element extraction (Sr, REE) was performed using AG 50W-X8 (200-400 mesh, Bio-Rad) resin and 2.5 N and 4.0 N HCl as eluant. Nd was separated from the REE group using teflon-coated HfEHP (Di-2-Ethylhexylphosphoric acid) and 0.24 N HCl as eluant. Maximum total procedural blanks (< 1 ng for Sr and 50 pg for Nd) were negligible. Pure element fractions were evaporated using a Re double filament assembly and run in static mode on a Thermo-Finnigan Triton TI TIMS. A mean ⁸⁷Sr/⁸⁶Sr ratio of 0.710250 ± 0.000004 (n = 8) was determined for the NBS987 (Sr) and a mean ¹⁴³Nd/¹⁴⁴Nd ratio of 0.511847 ± 0.000002 (n = 6) for the La Jolla (Nd) international standards during the period of investigation. Within-run mass fractionation was corrected (linear method) using values of ⁸⁸Sr/⁸⁶Sr = 8.3752, and ¹⁴⁶Nd/¹⁴⁴Nd = 0.7219, respectively.

4. Petrography

Lithologies of the SSAC include, (i) syenites representing the alkalinefelsic rocks of the complex, (ii) alkali gabbro, ijolite-melteigite and nepheline syenites (with modal clinopyroxene present up to 26.6% as dominant mafic constituent) corresponding to the alkaline-mafic rocks (iii) alkali pyroxenite representing ultramafic rocks and (iv) carbonatites. The modal compositions of representative samples of the studied lithologies are given in Table 1. Petrographically, syenites are coarse-grained and consist of K-feldspar, amphibole, clinopyroxene, plagioclase, and carbonates. Biotite, titanite, apatite, and opaque occur as accessory minerals. They show an overall hypidiomorphic granular texture (Fig. 3A) with local development of perthitic intergrowths. In some syenite samples, clinopyroxene grains occur as inclusion within melanite garnet, suggesting the earlier formation of clinopyroxene. Ijolite-melteigite rocks show coarse-grained, hypidiomorphic granular texture (Fig. 3B). Nepheline and clinopyroxene (in some samples, biotite, melanite, and carbonates) are present as major constituents. Titanite, apatite, and opaque constitute accessory phases. Development of melanite garnet at the expense of clinopyroxene suggests complex late-stage metasomatic reactions of earlier-formed mafic minerals with alkali rich fluids (Saha et al., 2011).

Alkali gabbro including shonkinite (melanocratic foid syenite) and malignite (mesocratic foid syenite) contains K-feldspar, clinopyroxene, and nepheline as major mineral constituents. Titanite, apatite, carbonates, and opaques are accessory phases. Nepheline syenites are characterized by coarse-grained, hypidiomorphic granular texture and essentially composed of K-feldspar and nepheline. Accessory minerals include biotite, titanite, apatite, and opaques. Poikilitic relationship between clinopyroxene and K-feldspar in shonkinite (Fig. 3C) and between nepheline and clinopyroxene in nepheline syenites (Fig. 3D) has been observed. Alkali pyroxenites are dominantly composed of aegirine-augite and aegirine, whereas K-feldspar, nepheline, biotite, titanite, apatite, and opaque minerals are present in subordinate amounts. In general, the studied alkali pyroxenites show cumulus texture where clinopyroxene occurs as cumulates and nepheline occupies the intervening spaces as intercumulus phase (Fig. 3E). Carbonatites predominantly comprise calcite, while clinopyroxene and biotite occur as major mafic constituents. In some carbonatite samples (SAJ 13A), apatite is present in proportions. The carbonatites of SSAC are mainly sovite with a coarse-grained, hypidiomorphic granular textural pattern (Fig. 3F). The chemical compositions of constituent mineral phases of SSAC have been reported by Saha et al. (2010a; 2011).

5. Whole rock geochemistry

5.1 Alkaline-silicate rocks

Major oxide compositions for different alkaline-silicate rocks from SSAC are given in Table Supplementary 1. Syenites are characteristically marked by high but restricted range of SiO₂ (59.5 wt. % to 61.9 wt. %), high Al₂O₃ (14.34 to 18.99 wt. %), low to moderate MgO (0.1-4 wt. %), CaO (0.25 to 4.35 wt. %), low content of MnO (0.07 to 0.13 wt. %) and TiO₂ (0.11 to 0.54 wt. %). P₂O₅ varies between 0.52 and 1.55 wt. %. and total alkali (Na₂O+ K₂O) content ranges from 12.45 to 14.73 wt. %. K₂O varies between 7.57 and 13.20 wt. % and is much higher than Na₂O, which ranges from 1.53 to 5.61 wt. %. K₂O/ Na₂O ratio ranges from 1.35 to 8.63 depicting the potash-rich character of the syenites. The agpaitic indices [A.I. = (Na₂O+ K₂O)/ Al₂O₃] for the syenites are >1 (ranging from 1.11 to 1.42) suggesting their agpaitic nature. The Mg# of the syenites ranges from 0.01 to 0.56. The studied ijolite-melteigite rocks are characterized by low to moderate SiO₂ content (ranging from 37.49 wt. % to 48.27 wt. %), moderate content of MgO (5.27 to 8.88 wt. %), moderate to high CaO (8.16 to 16.98 wt. %) and low content of MnO (0.10 to 0.50 wt. %). Moderated to high TiO₂ content ranges from 0.87 to 2.16 wt. % and P₂O₅ varies between 0.35 and 1.81 wt. %. Total alkali (Na₂O+ K₂O) content in ijolite-melteigite ranges from 3.24 to 11.41 wt. %, while Al₂O₃ ranges from 8.07 to 16.19 wt. %. K₂O varies between 1.35 and 9.32 wt. %, while Na₂O ranges from 1.51 to 7.33 wt. %. There is a gradual decrease in total alkali (Na₂O+ K₂O) content from melteigite (SAJ 19, SAJ 16, SAJ

10 and SAJ 17) to ijolite (SAJ 3, SAJ 23, SAJ 33 and SAJ 7) depicting an alkali enrichment trend from melteigite to ijolite. Further, a closer scan into the relative variations of K_2O/Na_2O ratios reveal that samples SAJ 3 and SAJ 23 (ijolite) and samples SAJ 19, SAJ 16 and SAJ 17 (melteigite) are marked by lower K_2O/Na_2O ratios (ranging from 0.38 to 0.71) than samples SAJ 33, SAJ 7 (ijolite) and SAJ 10 (melteigite) where K_2O/Na_2O ratios (ranging from 1.78 to 5.48) are much higher (Table Supplementary 1). These observations suggest a relative enrichment of soda over potash for the samples with lower K_2O/Na_2O ratios, while the higher K_2O/Na_2O ratios indicate a potash-rich character of ijolite-melteigite. The agpaitic indices [A.I. = $(Na_2O + K_2O)/Al_2O_3$] for samples SAJ 33, SAJ 7 (ijolite) and SAJ 19 (melteigite) are >1 (ranging from 1.07 to 1.12) suggesting their agpaitic nature. Samples SAJ 3, SAJ 23 (ijolite) and SAJ 16, SAJ 10 and SAJ 17 (melteigite) are distinctly miaskitic with agpaitic indices (A.I.) <1 (ranging from 0.59 to 0.96). The Mg# of ijolite-melteigite ranges from 0.36 to 0.59. Alkali pyroxenite and alkali gabbro rocks of SSAC have a variable silica composition with SiO_2 content ranging from 47.70 wt. % to 53.48 wt. % and they are characterized by moderate to higher abundances of MgO (5.49 to 10.02 wt. %) and CaO (12.13 to 18.36 wt. %); low content of MnO (0.17 to 0.35 wt. %) and low to moderate TiO_2 (0.29 to 1.26 wt. %). P_2O_5 varies between 0.34 and 3.74 wt. %. Total alkali ($Na_2O + K_2O$) content in alkali pyroxenite and alkali gabbro ranges from 5.52 to 9.03 wt. %, while Al_2O_3 ranges from 6.16 to 10.45 wt. %. K_2O varies between 1.58 and 7.08 wt. % and is relatively higher than Na_2O (1.50 to 3.94 wt. %). K_2O/Na_2O ratio ranges from 0.40 to 3.63 depicting the potash-rich character of the alkali pyroxenite and alkali gabbro rocks except one alkali pyroxenite sample (SAJ 36) which is relatively soda rich with $Na_2O > K_2O$ and K_2O/Na_2O ratio of 0.40. The agpaitic indices [A.I. = $(Na_2O + K_2O)/Al_2O_3$] for the alkali pyroxenite and alkali gabbro are >1 (ranging from 1.02 to 1.49) suggesting their agpaitic nature. The Mg# of these rocks ranges from 0.40 to 0.63. Nepheline syenites from SSAC exhibit a restricted range of silica abundances with SiO_2 content ranging from 50.10 wt. % to 55.08 wt. % with low MgO content (0.43 to 1.34 wt. %), moderate CaO content (3.21 to 7.29 wt. %) and low content of MnO (0.13 to 0.21 wt. %). TiO_2 ranges from 0.19 to 0.77 wt. % and P_2O_5 varies between 0.10 and 1.08 wt. %. Total alkali ($Na_2O + K_2O$) content in nepheline syenites ranges from 13.62 to 15.43 wt. %, while Al_2O_3 shows a much higher abundance ranging from 19.59 to 20.74 wt. %. K_2O ranges from 3.86 to 10.11 wt. %, while Na_2O varies between 5.32 and 9.79 wt. %. K_2O/Na_2O ratio in nepheline syenites ranges from 0.39 to 1.90 indicating that sample SAJ 25 ($K_2O/Na_2O = 1.90$) is potash-rich while samples SAJ 30 ($K_2O/Na_2O = 0.95$) and SAJ 32 ($K_2O/Na_2O = 0.39$) depict a relative soda enrichment over potash. The agpaitic indices [A.I. = $(Na_2O + K_2O)/Al_2O_3$] for the nepheline syenite samples SAJ 25 (A.I. = 1.19) and SAJ 30 (A.I. = 1.03) are >1 suggesting their

agpaitic nature while sample SAJ 32(A.I.= 0.95) shows a miaskitic nature. The Mg# of the nepheline syenites ranges from 0.10 to 0.25 depicting a much differentiated and evolved character.

Major oxide variations for alkali pyroxenite (alkaline-ultramafic), alkali gabbro, ijolite-melteigite, nepheline syenite (alkaline-mafic) and syenite (alkaline-felsic) from Samchampi-Samteran are plotted against their respective SiO₂ contents in Fig. 4. Critical evaluation of major oxide variation trends with respect to SiO₂ (Fig. 4) reveal that (i) Al₂O₃ and P₂O₅ show no perceptible trend (ii) total alkali ((Na₂O+ K₂O) systematically increases with rising SiO₂ and depict a positive correlation with the degree of differentiation while (iii) CaO and MgO show a negative trend with increasing SiO₂. These variation patterns (ii) and (iii) reflect magmatic differentiation.

On total alkali (Na₂O+K₂O) vs. silica (SiO₂) plot (Fig. 5A after Cox et al., 1979) for geochemical classification, the syenite samples cluster in field for syenites, ijolite-melteigite samples (except one) correspond to the ijolite field and nepheline syenite samples fall in the respective compositional field. All the samples belong to the alkaline field demarcated by the curved solid line after Irvine and Baragar (1971). The total alkali (Na₂O+K₂O) vs. silica (SiO₂) diagram (after McDonald and Katsura, 1964) (Fig. 5B) clearly shows that all the silicate rocks of SSAC distinctly occupy the “alkaline” field. Compositional plots of the studied rocks in Fig. 5C reveal that the alkali pyroxenite-alkali gabbro samples plot in the field of alkali basalt, while the ijolite samples dominantly fall within the field of miaskitic syenite with few samples exceeding the boundaries and falling between the fields of alkali basalt-miaskitic syenite and miaskitic syenite-agpaitic syenite. The melteigite samples correspond to nephelinite, while the nepheline syenites plot in the fields of agpaitic and miaskitic syenite. The syenites occupy alkali basalt and miaskitic syenite fields.

Trace element concentrations (including REE) of alkaline-silicate rocks from SSAC (Table Supplementary 1) suggest that these are distinctly characterized by elevated abundances of Large Ion Lithophile Elements (LILE; Rb, Sr, and Ba), and High Field Strength Elements (HFSE; Nb, Ta, Zr, Y, Hf, Th, U) that are consistent with compositions of alkaline igneous rocks (Dawson et al., 1995). The REE abundances are marked by high concentrations of LREE with relatively low HREE contents. ΣREE of the studied samples shows a wide range from 11.7 to 1050 ppm (Table Supplementary 1). Variations of Rb and Ba show positive correlation with SiO₂ while Y, Ni/Co and ΣREE exhibit decreasing trends with rising SiO₂ (Fig. 6) conforming to magmatic differentiation. No distinct variation trend is evident for Sr, Zr, Nb, Zr/Hf, Nb/Ta and Eu/Eu* (Fig. 6)

Chondrite-normalized REE patterns (Sun and McDonough, 1989) (Fig. 7) of the alkaline-silicate members indicate LREE enrichment and relatively lower abundances of HREE. (Ce/Yb)_N

values range between 3.69 and 69.22 (Table Supplementary 1) thereby suggesting a strong LREE/HREE fractionation. $(La/Sm)_N$ values varying between 0.86 and 5.74 are consistent with moderate to high LREE/MREE fractionation while the $(Gd/Lu)_N$ values ranging from 1.01 to 13.80 corroborate moderate to strong MREE/HREE fractionation. Primitive mantle normalized incompatible trace element abundance patterns for the alkaline-silicate rocks of SSAC (Sun and McDonough, 1989; Fig. 7) exhibit positive anomalies at Nb, Ta and negative anomalies at Th, K, P, Zr and Ti.

5.2 Carbonatites

Carbonatites represent the non-silicate member of SSAC. The studied samples exhibit a higher range of CaO abundances with CaO content ranging from 42.70 wt. % to 45.44 wt. % and moderate MgO content (4.63 to 5.20 wt. %). The carbonatites are characterized by relatively low contents of SiO₂ (6.07 to 7.81 wt. %), Al₂O₃ (1.21 to 1.30 wt.%) and total alkali (Na₂O+ K₂O) (1.57 to 1.78 wt. %). TiO₂ ranges from 0.42 to 0.64 wt. % and P₂O₅ varies between 0.07 and 0.72 wt. %. The low SiO₂, Al₂O₃, Na₂O and K₂O contents of the studied carbonatites are consistent with the major oxide compositions of most plutonic carbonatites (Woolley and Kempe, 1989). K₂O ranges from 1.35 to 1.42 wt. %, while Na₂O varies between 0.22 and 0.36 wt. %. K₂O/ Na₂O ratio in carbonatites (ranging from 3.94 to 6.14) reflects their potash-rich character. The agpaitic indices [A.I. = (Na₂O+ K₂O)/Al₂O₃] for the carbonatite samples (ranging from 2.00 to 2.13) are >1 suggesting their agpaitic nature. The Mg# of the carbonatites ranges from 0.55 to 0.77. In terms of their major oxide compositions, the Samchampi-Samteran carbonatites can be classified as calciocarbonatites with $CaO/(CaO+MgO+FeO+Fe_2O_3+MnO) > 0.8$ (Woolley and Kempe, 1989) and are compositionally akin to global calciocarbonatite (Woolley and Kempe, 1989) and those from Chilwa (Karmalkar et al., 2010), Amba Dongar (Gwalani et al., 1993) and Sung Valley (Srivastava et al., 2005) the alkaline complexes.

The trace element compositions of Samchampi-Samteran carbonatites are characterized by high contents of LILE (Ba, Sr) HFSE (Nb, Ti, Zr, Th) and LREE (Table Supplementary 1). Chondrite normalized REE patterns of the Samchampi-Samteran carbonatites (Sun and McDonough, 1989; Fig. 7A) with their elevated $(La/Lu)_N$ (74.56 to 112.94), $(La/Yb)_N$ (73.53 to 142.18) and $(Ce/Yb)_N$ (ranging from 30.31 to 89.96) values (Table Supplementary 1) reflect LREE enrichment and LREE/HREE fractionation. In addition to this, $(La/Sm)_N$ (4.71 to 6.68) and $(Gd/Lu)_N$ (7.21 to 10.01) values (Table Supplementary 1) corroborate LREE/MREE and MREE/HREE fractionations respectively. The REE abundances of these carbonatites are characteristically higher than that of the associated alkaline-silicate rocks (Fig. 7). Primitive mantle-normalized multi-element patterns (Sun

and McDonough, 1989) for Samchampi-Samteran carbonatites (Fig. 7) exhibit distinct positive anomalies at Nb, Ta, Sm, Nd and negative Zr anomalies. The average Nb concentration in the Samchampi-Samteran carbonatites (avg. Nb= 6992.1 ppm) (Table Supplementary 1) falls within the range of average calciocarbonatite (1-15000 ppm; Woolley and Kempe, 1989).

5.3 Sr and Nd isotope systematics

Results of Sr and Nd isotopic compositions of a representative sample suite from SSAC are given in Table 2. Initial Sr and Nd isotope ratios, along with respective epsilon values were calculated assuming an emplacement age of 105 Ma (Acharyya et al., 1986; Heaman et al., 2002; Srivastava et al., 2005). Epsilon values are calculated using present-day ratios of $^{87}\text{Sr}/^{86}\text{Sr} = 0.7045$ (De Paolo, 1988) and $^{87}\text{Rb}/^{86}\text{Sr} = 0.0827$ (De Paolo, 1988) for Bulk Silicate Earth (BSE); $^{143}\text{Nd}/^{144}\text{Nd} = 0.512638$ (Goldstein et al., 1984) and $^{147}\text{Sm}/^{144}\text{Nd} = 0.1967$ (Jacobsen and Wasserburg, 1980) for Chondritic Uniform Reservoir (CHUR). The studied samples of SSAC have $^{87}\text{Sr}/^{86}\text{Sr}_i$ and $^{143}\text{Nd}/^{144}\text{Nd}_i$ ratios ranging from 0.705562 to 0.709416 and from 0.512187 to 0.512449, respectively.

6. Discussion

6.1 Petrogenesis of silicate and carbonatite rocks

The origin of carbonatites and their spatial, temporal and genetic relationship with the associated alkaline-silicate rocks is complex and a topic of worldwide petrological interest in recent years (Bell et al., 1998; Gittins and Harmer, 2003; Mitchell, 2005; Srivastava et al., 2005; Chen and Simonetti, 2013). Proposed models for the generation of carbonatites include: i) derivation of carbonatites by direct melting of a carbonate-bearing mantle-source (Wyllie and Huang, 1976; Gittins, 1989; Dalton and Presnall, 1998; Bailey et al., 2001), ii) carbonatites evolving by immiscible separation from a silicate-carbonate melt (Freestone and Hamilton, 1980; Kjarsgaard and Hamilton, 1988; Brooker, 1998), and iii) crystal fractionation of a carbonated alkali silicate melt (Veksler et al., 1998). In the present study, the genesis of Samchampi-Samteran carbonatites and the petrogenetic link between the alkaline-silicate rocks and carbonatites of SSAC has been assessed in the light of trace element and REE geochemistry and radiogenic isotopic signatures.

Field relationships suggest that the ijolite-melteigite suite of rocks intrude the syenite, while the alkali pyroxenite-alkali gabbro occur as inliers within the ijolite-melteigite rocks of SSAC, whereas nepheline syenite intrudes the ijolite-melteigite rocks as late intrusives with sharp contacts. Rocks types that are intermediate in composition between the ijolite-melteigite and nepheline syenite are lacking. The Mg# values (Table Supplementary 1) suggest that the alkaline-silicate rocks are

devoid of crystal cumulation effects. The trace element variation plots for the alkaline-silicate members are scattered and do not show any appreciable trend (Fig. 6). If the Samchampi-Samteran rocks were formed by fractional crystallization, then the most viable crystallization sequence would have given rise to pyroxenite, ijolite, and syenite, while carbonatites would represent the crystallized residual liquid fraction. However, a simple fractional crystallization model, using Sr concentration variation in alkaline rocks (Albarede, 1995), predicts an unreasonably high Sr concentration (~15000 ppm, which is much higher than the average concentration observed in carbonatites) for the residual carbonate melt (Ray et al., 2000). Considering the fact that carbonatites usually constitute a small fraction of the total mass of exposed rock in a plutonic alkaline-carbonatite complex (Barker, 1989), it may be inferred that SSAC carbonatites of the present study did not crystallize from a residual melt. These observations suggest that the alkaline silicate rocks of SSAC were not co-magmatic and their derivation cannot be related to simple fractional crystallization involving a single parental melt. The highly variable Sr-Nd isotope compositions (Table 2) for these rocks cannot be attributed to closed system crystal fractionation and this contention further substantiates the role of more than one parental melt in the generation of SSAC.

In many alkaline igneous complexes of the world, silicate-silicate liquid immiscibility has been envisaged as a dominant petrogenetic process (Eby, 1975; 1979; Philpotts, 1982; Subrahmanyam and Leelanandam, 1989; Halama et al., 2005; Doroshkevich et al., 2010; Mukhopadhyay et al., 2011; Sensarma and Palme, 2013). HFSE compositions serve as an effective tool to evaluate the role of liquid immiscibility in alkaline magmas. These elements (HFSE) cannot obtain co-ordination polyhedra or oxygen in silica-rich polymerized melts and are normally partitioned into silica-poor, less polymerized mafic melts (Hess, 1971; Warner, 1973). It has also been suggested that the liquid immiscibility field is enhanced by P^{5+} and Ti^{4+} cations in the melt (Visser and Koster Van Grove, 1979) and consequently, the felsic melts are relatively depleted in HFSE, P and Ti relative to the mafic melts (Rajesh, 2003). Experimental observations and theoretical models have provided evidence supporting the trace element partitioning between two immiscible silicate liquids during alkaline magmatism (Roedder, 1951; Hess and Rutherford, 1974; Watson, 1976). However, considering the scattered trace element variations and discrete isotopic compositions for the alkaline-silicate rocks, we discount the liquid immiscibility model for SSAC. Therefore, field observations, geochemical characteristics and isotopic signatures invalidate fractional crystallization or liquid liquid immiscibility as viable petrogenetic processes for the generation of alkaline-silicate rocks of SSAC and suggest their derivation from different batches of parental melts generated by repeated episodes of mantle melting. Elevated abundances of LILE and

REE signatures with pronounced LREE/HREE fractionation (Table Supplementary 1) reflect low degree partial melting of a metasomatized garnet peridotite that generated alkali-basaltic melts parental to the alkaline-silicate rocks of SSAC. The nepheline normative compositions of these alkaline-silicate rocks combined with these geochemical signatures conform to carbonated garnet peridotite melting under ~ 3 GPa pressure with CO₂ as a dominant metasomatizing agent (Hirose, 1997; Hirschmann et al., 2003).

There has been much debate about whether carbonatite magmas are derived through liquid immiscibility of a silica-undersaturated magma (Schultz et al., 2004) or whether they are derived by direct partial melting of a carbonated peridotite mantle (Harmer and Gittins, 1998; Petibon et al., 1998; Chakhmouradian, 2006). It has been experimentally established that under almost all conditions the Ba/La ratio should be higher in an immiscible carbonatite liquid relative to its conjugate silicate fraction (Hamilton et al., 1989; Harmer, 1999; Srivastava et al., 2005). For SSAC, the silicate members have higher Ba/La ratio (2.39-106.11, avg. 19.32) than the carbonatite (1.04-1.15, avg. 1.09) (Table Supplementary 1; Fig. 8). The REE distribution pattern between silicate and carbonatite rocks provides a good test of the liquid immiscibility mechanism. It has been demonstrated that if both the silicate and carbonatite fractions are derived from a single parent melt through liquid immiscibility, then the silicate rocks will have a higher (Ce/Yb)_N ratio than carbonatite implying steeper REE patterns and more LREE/HREE fractionation in the silicates (Macdonald et al., 1993). But in this study, the carbonatites have much higher (Ce/Yb)_N ratio (30.31-89.96, avg.64.85) than the alkaline-silicate rocks [(Ce/Yb)_N ratio:3.69-69.22, avg. 24.55] (Table Supplementary 1), which point towards relatively higher degree of LREE/HREE fractionation in carbonatites than the alkaline-silicate rocks of SSAC. The REE-enriched character of the carbonatites with respect to the alkaline-silicate rocks is further reflected in chondrite-normalized REE patterns (Fig. 7). Thus, REE signatures and LREE/HREE partitioning relationships provide strong evidence against the Samchampi-Samteran carbonatites being derived by liquid immiscibility. The distinct isotopic signatures and geochemical parameters for the studied carbonatites and alkaline-silicate rocks are inconsistent with their derivation by liquid immiscibility or fractional crystallization from common parent magma. Rather, generation of carbonatites and alkaline silicate rocks as separate mantle melts from episodic melting events appears much reasonable (Poletti et al., 2016). Therefore, considering these parameters, a liquid immiscibility origin of the carbonatite is untenable and it is proposed that the Samchampi-Samteran carbonatite are derived from primary carbonatite magmas generated by partial melting of a carbonated mantle peridotite. The SSAC is broadly similar to the alkaline-carbonatite complexes of Africa such as Napak, Kerimasi, Shombole,

Spitskop (Harmer and Gittins, 1998) and Mountain Pass ultrapotassic and carbonatite intrusive suite, California (Poletti et al., 2016) where that petrogenetic relationships between carbonatites and alkaline silicate rocks discard the role of liquid immiscibility in their evolution history and favour a model involving partial melting of carbonated mantle peridotite.

Therefore, it is envisaged that the petrogenetic evolution of Samchampi-Samteran alkaline complex is governed by the following broad parameters (a) metasomatic wehrlitization and carbonization of garnet lherzolite (Harmer 1999) (b) multiple episodes of low degree partial melting of this metasomatically enriched, mantle wehrlite generating isotopically distinct batches of parental ultrabasic alkaline magmas that formed the alkaline-silicate rocks (c) late stage derivation of carbonatite by direct, lower degree (0.1-0.5%) melting of metasomatized and carbonated mantle peridotite. The variable Sr-Nd isotopic compositions for silicates and carbonatite of SSAC (Table 2) are attributed to discrete batches of parental melt generated from different mantle-melting events of an isotopically heterogeneous mantle.

6.2 Implications on mantle source, plume signature and plume-lithosphere interaction

The incompatible trace element abundances for rocks from the SSAC, as evidenced by their pronounced enrichments in LILEs, LREEs, and HFSEs combined with relative depletion in HREEs, suggest an enriched mantle source for the generation of parental melts. It has been envisaged that positive Nb anomalies with enrichment in incompatible trace elements are the prominent geochemical signatures of plume-related magmas of both oceanic and continental realms (Safonova, 2009; Safonova et al., 2008; Simonov et al., 2015). Primitive mantle-normalized multi-element patterns for SSAC rocks (except two samples of syenite), marked by positive Nb-Ta anomalies, negative K, Th and Sr anomalies (Fig. 7), collectively attest to derivation of alkaline-carbonatite magmas from a plume-related OIB-type mantle source in an intraplate, rift-controlled tectonic setting (Nelson et al., 1988; Verhulst et al., 2000; Pilet et al., 2008; 2010; 2011). The LREE-Nb-Ta enrichment for the alkaline-carbonatite rocks of SSAC are typical of those found in plume-derived OIB melts thereby implying plume signature in the source mantle for SSAC lithologies. Inter-element relationships in LREE-Nb-Th systematics marked by high Nb contents, positive Nb-Ta anomalies relative to Th and La, $Nb/La > 1$ and $Nb/Th > 1$ substantiate the contribution of mantle plume towards the origin of the melts parental to the alkaline-silicate rocks and carbonatite of SSAC. Further, Nb-Ta enrichment and $Nb/La > 1$ are consistent with the presence of a recycled subduction component in the plume source (Weaver, 1991; Cabral et al., 2013). Positive Nb-Ta anomalies on mantle normalized multi-element patterns, LILE and LREE enrichments but no HFSE depletion relative to primitive mantle are similar to OIB-type magma and suggest derivation of parent melts from a mantle plume

source containing subduction-processed, ancient, recycled slab materials (Dai et al., 2014). The conjunction of positive Nb-Ta anomalies with Nb/Th >1 and Nb/La >1 negate the role of crustal contamination and are consistent with recycling of subduction-processed, residual basaltic oceanic lithosphere into the mantle prior to plume-upwelling and generation of magma parental to the studied alkaline-carbonatite rocks (Hofmann and White, 1982; Lassiter and DePaolo, 1997; Song et al., 2008; Sleep, 2006; White, 2010).

The SSAC samples are characterized by relatively high $^{87}\text{Sr}/^{86}\text{Sr}_{\text{initial}}$ ratios ranging from 0.705562 to 0.707368, while $^{143}\text{Nd}/^{144}\text{Nd}_{\text{initial}}$ isotopic compositions vary between 0.512187 and 0.512449 (Table 2). The variations of $^{87}\text{Sr}/^{86}\text{Sr}_{\text{initial}}$ and $^{143}\text{Nd}/^{144}\text{Nd}_{\text{initial}}$ values of representative samples are consistent with an isotopically heterogeneous mantle source. The $\text{Sr}_{\text{initial}}$ and $\text{Nd}_{\text{initial}}$ (105Ma) isotopic compositions of SSAC are suggestive of parent magma generation from an enriched mantle source. The ϵ_{Sr} and ϵ_{Nd} isotopic signatures of these alkaline-carbonatite rocks attest to a plume-related EM-II affinity. It is observed that the carbonatite and alkaline-silicate samples plot within the enriched quadrant of the $^{143}\text{Nd}/^{144}\text{Nd}_{\text{initial}}$ vs. $^{87}\text{Sr}/^{86}\text{Sr}_{\text{initial}}$ diagram (Fig. 9A). This variation of $^{87}\text{Sr}/^{86}\text{Sr}_{\text{initial}}$ and $^{143}\text{Nd}/^{144}\text{Nd}_{\text{initial}}$ values of alkaline-silicate and carbonatite samples may be equated with their derivation from different batches of parental magma which was generated by periodic melting of an isotopically heterogeneous source with enriched mantle signatures. In terms of $^{143}\text{Nd}/^{144}\text{Nd}_{\text{initial}}$ vs. $^{87}\text{Sr}/^{86}\text{Sr}_{\text{initial}}$ variations (Fig. 9B), the plots for syenite, melteigite, alkali gabbro, and carbonatite samples overlap with the field of Kerguelen Plateau Basalts. The alkali pyroxenite and ijolite samples plot near the enriched mantle (EM II) field. Thus, the $\epsilon_{\text{Sr}} - \epsilon_{\text{Nd}}$ isotopic signatures of SSAC suggest a possible genetic link between the SSAC and Kerguelen plateau basalts, and point towards the involvement of a Kerguelen plume-related enriched mantle (~EM II) source.

The context of alkaline-carbonatite magmatism in rift-controlled, intraplate tectonic regimes raises two stimulating questions as to whether the parental melts are generated within the continental lithosphere or whether they are derived from deeper parts of the mantle with the lithosphere playing an important role in trapping volatile rich fluids (Marzoli et al., 2000; Grange et al., 2010; Bell and Simonetti, 2010). The emplacement of highly silica-undersaturated magmas comprising a wide compositional spectrum ranging from alkaline ultramafic-mafic to alkaline felsic lithologies and carbonatites provide the best *prima facie* evidence of metasomatism, volatile activity and melt-enrichment processes operating in the mantle in open-system conditions (Pilet et al., 2008; Martins et al., 2010). The analogous geochemical and isotopic characteristics of small volume of alkaline melts from continents and alkali basalts from small oceanic islands invoke (i) related mantle processes and sources for their genesis and (ii) melting of both asthenospheric and lithospheric mantle (Nelson et

al., 1988; McKenzie and O'Nions, 1995). Noble gas isotopic studies suggest that for alkaline-carbonatite magmatism in intracontinental setting, the metasomatism of subcontinental lithospheric mantle is stimulated by an upwelling plume carrying asthenospheric mantle (Wyllie et al., 1990; McKenzie and O'Nions, 1995).

Pronounced LILE and LREE enrichment of the investigated rocks together with steep LREE/HREE profile and strong HREE fractionation provide evidence for parent magma generation from low degree partial melting of a metasomatized mantle with retention of garnet in the source. HFSE enrichment of SSAC rocks is ascribed to recycled subduction components in the plume magmatism that was involved in parent melt generation, while LILE and LREE enrichments reflect contribution from a metasomatized lithospheric mantle in their genesis (Downes et al., 2005; Pilet et al., 2005; 2011; Dai et al., 2014). High Zr/Hf values (>36) are the diagnostic feature of metasomatized mantle (Dupuy et al., 1992; Rudnick et al., 1993; Dostal and Chatterjee, 2000; Kurkcuoglu, 2010). In the present study, the elevated Zr/Hf values (>36) of the alkaline-silicate (Zr/Hf: avg. 55.86) rocks and carbonatites (Zr/Hf: avg. 176.68) distinctly fingerprint the role of a metasomatized mantle in the evolution of this complex. The isotopic variations for alkaline-silicate rocks and carbonatites may be attributed to mantle heterogeneity and various extents of plume-lithosphere interaction (Wyllie et al., 1990; McKenzie and O'Nions, 1995; Ma et al., 2011). It is thus inferred that the origin of parent magmas for SSAC in a rift-controlled continental regime was related to (i) a mantle plume carrying recycled subduction components from lower mantle (ii) decompression melting of upwelling plume head and interaction with lithosphere (iii) metasomatism of the subcontinental lithospheric mantle. Therefore, the enriched mantle source for SSAC is equated with interaction of a plume-derived melts with metasomatized sub-continental lithospheric mantle in an intracontinental rift-setting.

6.3. Comparison with Sung, Jasra, Mawpyut and Swangkre-Rongmil complexes

A brief account of the isotopic compositions, mantle source characteristics and geochronological data of Sung Valley, Jasra, Samchampi-Samteran, Mawpyut and Swangkre-Rongmil complexes is listed in Table 3. The LILE, HFSE and LREE enrichments of the alkaline-silicate rocks and carbonatites are in compliance with the involvement of a plume-related OIB-type mantle marked by contribution recycled subduction components. The Sr-Nd isotopic compositions of Sung Valley, Jasra, Samchampi-Samteran, Mawpyut (Table 3) reflect contribution from enriched mantle components in the mantle source (Fig. 9B) and the enriched isotopic signature is supportive of mantle heterogeneity. This heterogeneity is generally attributed to the entrainment of lower mantle material through the upwelling of deep mantle plumes (Hoernle et al., 1995; Harmer and Gittins,

1998; Srivastava et al., 2005). Sung Valley is the best attended differentiated complex of Northeastern India which has attracted the attention of many geologists since long. Nepheline syenite and ijolite from Sung Valley have distinct EM-II mantle source, while carbonatites have originated by mixing of HIMU and EM-II (Srivastava et al., 2005). Petrological details of Jasra complex have been mostly worked out by Srivastava and Sinha (2004a;2004b; 2007). Gabbro, syenite and pyroxenite appear to have been derived from different parental melts but each of the rock types bears appreciable evidence of magmatic differentiation. Geochemical signatures coupled with isotopic compositions of alkaline ultramafic-mafic rocks of Jasra corroborate an OIB-type mantle source for the generation of parent magma. Radiogenic isotopic signatures further suggest a mixing of mantle components like HIMU and enriched mantle for these rocks (Table 3). The alkaline ultramafic-mafic rocks of Jasra are not cogenetic and reflect multiple melt generation processes for their genesis. In this study, enriched Sr-Nd isotopic signatures (Tables 2 and 3) of the alkaline-carbonatite rocks attest to a plume-related enriched mantle (~EM II) source in relation to the origin of Samchampi-Samteran alkaline complex. Large variations in isotopic data invoke periodic melting of an isotopically heterogeneous, metasomatized mantle and generation of isotopically distinct melt batches that were parental to the alkaline-silicate rocks and carbonatites of Samchampi-Samteran that show no genetic coherence. No genetic relation between the alkaline silicates and carbonatites has been envisaged for Sung Valley and Samchampi-Samteran thereby indicating distinct genetic history for the carbonatites. The isotopic compositions of cumulate and non-cumulate rocks of Mawpyut show a continental flood basalt affinity and attest to an enriched mantle source involving EM I/EM II/HIMU components (Chaudhuri et al., 2014). Geochemical characteristics of the mafic dykes of Swangkre-Rongmil, marked by elevated HFSE abundances, show their affinity to plume-related OIB-type source mantle (Srivastava and Sinha, 2004 a; 2004b).

The $^{87}\text{Sr}/^{86}\text{Sr}_{\text{initial}}$ and $^{143}\text{Nd}/^{144}\text{Nd}_{\text{initial}}$ isotopic compositions of Samchampi-Samteran rocks (Tables 2 and 3) are comparable with the range of Sr and Nd isotopic compositions of Sung Valley, Jasra and Mawpyut complexes (Figs. 9B and 10). For the ijolite-melteigite rocks of SSAC, the $^{87}\text{Sr}/^{86}\text{Sr}_{\text{initial}}$ and $^{143}\text{Nd}/^{144}\text{Nd}_{\text{initial}}$ ratios depict a close resemblance with the Sr-Nd isotopic compositions of the Sung Valley ijolites (Srivastava et al., 2005). Veena et al. (1998) suggested that the Sung Valley carbonatites derived from an enriched mantle source with an EM II signature. The enriched Sr-Nd signatures of Samchampi-Samteran carbonatites also indicate involvement of a mantle source carrying EM II component. Thus, the overall enriched Sr-Nd isotopic characters reveal an isotopic coherence among Samchampi-Samteran, Sung Valley and Jasra alkaline complexes (Fig. 9B). This

distinct isotopic character has been ascribed to a mantle plume carrying EM II signature (Veena et al., 1998).

6.4 Correlation with Sylhet Traps and link to Kerguelen plume

Fig.10 depicts the ϵ_{Nd} vs. $^{87}Sr/^{86}Sr_{initial}$ plots of Samchampi-Samteran samples together with the different lithologies from Mawpyut (Chaudhuri et al., 2014), Jasra (Srivastava and Sinha, 2004a), Sung Valley (Srivastava et al., 2005) complexes and fields for Kerguelen plateau basalts, Rajmahal tholeiites and Sylhet Trap basalts studied from Cherrapunji and Mawsinram-Baylot sections (Michard et al., 1986; Dosso et al., 1988; Storey et al., 1992; Mahoney et al., 1995; Ghatak and Basu, 2011; 2013). The Sr and Nd isotopic data for the Rajmahal basalts define two distinct groups: Group I with $^{87}Sr/^{86}Sr_{initial}$ and ϵ_{Nd} values ranging from 0.7037 to 0.7053 and 5.1 to 2.9 and Group II with 0.7064 to 0.7075 and -1.5 to -4.4, respectively (Coffin et al., 2002). The syenite, melteigite and alkali gabbro samples of SSAC correspond to the field of Kerguelen plateau basalts (K1 Site 747), while alkali pyroxenite and ijolite plot in between the fields of K1 Site 738 and Group II Rajmahal tholeiites. The carbonatite of SSAC corresponds to the field of Group II Rajmahal tholeiites. The $^{87}Sr/^{86}Sr_{initial}$ and $^{143}Nd/^{144}Nd_{initial}$ compositions of the studied alkaline-carbonatite rocks plot within the range of Sr-Nd isotopic ratios derived for Sylhet Trap basalts from Cherrapunji and Mawsynram-Baylot sections (Ghatak and Basu, 2011). High $^{87}Sr/^{86}Sr_{initial}$ ratios and negative ϵ_{Nd} values of SSAC and Group II Rajmahal tholeiites reflect their origin from an enriched mantle source. Therefore, the ϵ_{Nd} vs. $^{87}Sr/^{86}Sr_{initial}$ variations of the Samchampi-Samteran samples are consistent with the interpretation that the studied samples display isotopic ratio similarities to those for the Kerguelen plateau basalts, Rajmahal tholeiites (Group II) and Sylhet Trap basalts and hence suggest a genetic link. A U-Pb age of 105.2 ± 0.5 Ma was obtained by Heaman et al. (2002) on baddeleyite from the Jasra complex; U-Pb ages of 103.9-111.6 Ma were obtained for Sung Valley by Srivastava et al. (2005) and a fission-track age of 105 Ma was determined for SSAC by Acharyya et al. (1986), while K-Ar dating of a lamprophyre dyke from Swangkre-Rongmil has yielded 107 Ma age. Therefore, Jasra, Sung Valley and Samchampi-Samteran intrusive complexes post-date the Rajmahal and Sylhet Traps, which have $^{40}Ar-^{39}Ar$ ages of ~115-116 Ma (Baksi, 1995; Ray et al., 2005). The geochronological data of these complexes (Table 3) suggest that (i) they post-date the Rajmahal and Sylhet Traps, which have $^{40}Ar-^{39}Ar$ ages of ~115-116 Ma (Baksi, 1995; Ray et al., 2005) (ii) they were contemporaneous in terms of their genesis and emplacement and (iii) furthermore, the age data of Sung Valley, Jasra, Samchampi-Samteran and Swangkre-Rongmil are consistent with basalts from Kerguelen Plateau (110-119 Ma), Broken Ridge (100 Ma), Naturaliste Plateau (100.6 ± 1.2 Ma) and Rajmahal-Sylhet (105-118 Ma). A Kerguelen plume origin has been

proposed for the Sylhet and Rajmahal basalts (Ray et al., 1999; Kent et al., 2002; Mahoney et al., 1992; Heaman et al., 2002; Coffin et al., 2002; Duncan, 2002, Ghatak and Basu, 2011, 2013). Therefore, these implications reflect that SSAC of Mikir Hills is spatially, temporally and geochemically coherent with Sung Valley and Jasra alkaline complexes of Shillong Plateau and represents late-stage differentiation of Sylhet Traps which in turn has a genetic association with Kerguelen plume magmatism in north-eastern India.

The Kerguelen Plateau, (together with the Broken Ridge and associated igneous rock complexes from northeastern India, Australia and Antarctica) constitutes the Kerguelen Large Igneous Province (LIP), which formed as a result of widespread Cretaceous magmatism in the Southern Indian Ocean in response to Kerguelen mantle plume hotspot activity (Mahoney et al, 1983; Davies et al., 1989; Storey et al, 1992; Duncan and Storey, 1992; Nicolaysen et al, 2001; Kent et al, 2002; Coffin et al, 2002). The Kerguelen mantle plume system represents various modes of magmatism ranging from continental flood basalt volcanism to submarine plateau volcanism spanning over a period of upto ~132 Ma (Coffin et al., 2002). The emplacement of Cretaceous flood basalts on the rifted continental margins of eastern and northeastern India (Rajmahal-Sylhet flood basalts), western Australia (Bunbury-Naturaliste plateau basalts) and eastern Antarctica can be attributed to the melting of a starting plume head, the remnant of which (i.e. the plume tail) is now present as a hotspot beneath the Kerguelen Islands in the Indian Ocean (Storey et al, 1992; Muller et al., 1993; Frey et al., 2000; Kent et al., 2002). The mafic-alkaline intrusive rocks exposed in parts of north eastern India and east Antarctica (Rodak Lake alnoites) are considered to be contemporaneous with these flood basalts and are manifestations of various differentiation phases of plume-fed CFB magmatism (Ray et al., 1999; Ingle et al., 2002).

In northeastern India, the Sylhet Traps are exposed in a narrow, 80 km long and 4 km wide east-west trending belt and it is located along the southern margin of the Shillong Plateau, having a maximum thickness of 550-650m (Mazumdar, 1986). The Sylhet Traps have been envisaged to be the continuation of Rajmahal Traps, occurring approximately 550km west in eastern India. Ar-Ar geochronology has linked the Sylhet Traps with the Rajmahal Traps and these flood basalts have been correlated with the Kerguelen plume activity. Thus, the Bengal (covered by the Gangetic alluvium), Sylhet (exposed ~400 km east of Rajmahal) and Rajmahal (exposed) Traps, formed a single flood basalt province initially covering $\sim 2 \times 10^5$ km² area in the eastern and northeastern Indian subcontinent, recording the first manifestation of Kerguelen plume activity on the Indian plate around 117 Ma ago (Baksi, 1995; Segev, 2002). The Bengal-Sylhet-Rajmahal basalts (BSRB) comprise quartz tholeiites, alkali basalts and andesites which are linked to a variety of alkaline

igneous rocks including pyroxenites, ijolites, lamproites, lamprophyres and carbonatites that occur as intrusions in north-eastern India and east Antarctica (Storey, 1995; Courtillot et al., 1999; Segev, 2002).

During the Late Jurassic-Early Cretaceous, the of E-W trending Brahamaputra and Dauki fault systems in northeastern India broke the Shillong Plateau along its southern margin and acted as a fissure for concomitant extrusion of Sylhet Trap flood basalts and intrusive magmatic activities followed along the lineaments resulting in the isolated emplacements of ultramafic-mafic-alkaline-carbonatite complexes in Shillong Plateau and Mikir Hills (Gupta and Sen, 1988; Nandy, 2001). Thus, the eruption of Sylhet Trap flood basalts and associated differentiation centres (manifested in terms of ultramafic-mafic-alkaline-carbonatite intrusions) can be relegated to crustal extensions and development of rift zones in an intraplate continental setting. The available $Sr_{initial}$ and $Nd_{initial}$ (105 Ma) isotopic compositions and geochronological data of the Sung Valley, Jasra, Mawpyut, Samchampi-Samteran and Swangkre-Rongmil complexes are in agreement with those of Rajmahal tholeiites (Group II), Sylhet Traps and Kerguelen plateau basalts. A rift- controlled, continental, intraplate environment has been suggested (Fig. 11) for the emplacement of SSAC and this is also consistent with the regional tectonic framework. The evolution of SSAC is relegated to multiple episodes of low degree partial melting of an isotopically heterogeneous, metasomatized mantle source carrying both plume and lithospheric components.

7. Conclusion

- The evolution of metasomatically enriched, carbonated mantle peridotite and generation of alkaline magmas for SSAC involved two stages. In the first stage, decompression melting of an ascending mantle plume carrying recycled subduction components generates CO_2 rich fluids and melts enriched in HFSE and REE and volatile components. These melts, derived from an upwelling plume head, have very low viscosities; rapidly penetrate the lithospheric mantle and serve as a dominant metasomatizing agent. In the process of mantle metasomatism, the metasomatic fluids interacts with the mantle garnet lherzolite, consumes orthopyroxene (lherzolite), transforms it to metasomatic clinopyroxene and olivine and provides Al, Fe and Si, necessary for the crystallization of silicate minerals. In this process, the lherzolitic mantle is metasomatized to fluid enriched, carbonated, wehrlitic mantle. In the second stage, that low-degree partial melting (0.1-3%) of this metasomatized, alkaline wehrlite produces ultrabasic alkaline silicate magma.

- LILE, HFSE and LREE enrichment of the alkaline-silicate rocks and carbonatites of SSAC suggest involvement of plume-related OIB-type mantle and interaction of plume-derived melts with metasomatized lithospheric mantle.
- Pronounced LREE enrichment and HREE fractionation invoke low degree of partial melting of an enriched garnet peridotite mantle comprising plume and metasomatized lithospheric mantle components. Periodic melting of this enriched, metasomatized mantle source generated isotopically distinct batches of parental melts which account for large variations in trace element and isotopic compositions of SSAC.
- Sr-Nd isotopic signatures attest to the role of an isotopically heterogeneous, plume-related enriched mantle (EM II) component marked by contribution from recycled subduction component.
- The variable Sr-Nd isotopic compositions for silicates and carbonatite of SSAC account for periodic mantle-melting events of an isotopically heterogeneous mantle generating discrete batches of parental melts.
- The overall geochemical and isotopic signatures for SSAC (representing integrated part of Cretaceous alkaline-carbonatite magmatism of Shillong Plateau-Mikir Hills) strongly suggest its genetic linkage with Kerguelen plume-fed Rajmahal-Sylhet flood basalts.
- **Acknowledgements**

AS is grateful to the Director, CSIR-National Institute of Oceanography and Head, Geological Oceanography Division, CSIR-National Institute of Oceanography for their encouragement, support and permission to publish this work. Monika Horschinegg is thanked for performing the Sr and Nd isotope analyses. The authors thank the editor and two anonymous reviewers for their insightful comments and valuable suggestions which have greatly improved the quality of the manuscript. This is NIO's contribution No. XXXX.

References

- Acharyya, S.K., Mitra, N.D., Nandy, D.R., 1986. Regional geology and tectonic setting of Northeast India and adjoining region. Geological Survey of India Memoir 119, 6-12.
- Albarede, F., 1995. Introduction to geochemical modeling. Cambridge University Press, London, 543p.

- Baksi, A. K., 1995. Petrogenesis and timing of volcanism in the Rajmahal flood basalt province, Northeastern India. *Chemical Geology* 121, 73-90.
- Balaram, V., Gnaneshwar Rao, T., 2003. Rapid determination of REE and other trace elements in geological samples by microwave acid digestion and ICP-MS. *Atomic Spectroscopy* 24, 206-212.
- Balaram, V., 1992. Effect of concomitant elements on the analyte signals in ICP-MS - A case study. In: Bhattacharaya, K.G. (Ed.), *Proceedings of the National Seminar on Modern Trends in Analytical techniques: Applications in Chemistry*, Guwahati University Press 9, pp. 162-175.
- Bailey, D.K., 1993. Carbonate magma. *Journal of Geological Society of London* 150, 637-651.
- Bailey, J.C., Gwozdz, R., Rose-Hansen, J., Sorensen, H., 2001. Geochemical overview of the Ilímaussaq alkaline complex, South Greenland. *Geology of Greenland Survey Bulletin* 190, 35-53.
- Barker, D.S., 1989. Field relations of carbonatites. In: Bell, K. (Ed.) *Carbonatites: Genesis and Evolution*, Unwin Hyman, London, 38-69.
- Basu, A.R., Renne, P.R., Das Gupta, D.K., Teichman, F., Poreda, R.J., 1993. Early and late alkali igneous pulses and a high ^3He plume origin for the Deccan flood basalts. *Science* 261, 902-906.
- Bell, K., 2001. Carbonatites: Relationships to mantle plume activity. In: Ernst RE and Buchan KL (eds.) *Mantle Plumes: Their Identification Through Time*, Geological Society of America Special Paper 353, 267-290.
- Bell, K., Blenkinsop, J., 1989. Neodymium and strontium isotope geochemistry of carbonatite. In: Bell, K. (Ed.), *Carbonatites: Genesis and Evolution*, Unwin Hyman, London, pp. 278-300.
- Bell, K., Simonetti, A., 2010. Source of parental melts to carbonatites- critical isotopic constrains. *Mineralogy and Petrology* 98, 77-89.
- Bell, K., Kjarsgaard, B. A., Simonetti, A., 1998. Carbonatite-into the Twenty-First Century. *Journal of Petrology* 39, 1839-1845.
- Bell, K., Simonetti, A., 1996. Carbonatite magmatism and plume activity: implications from the Nd, Pb and Sr isotope systematic of Oldoinyo Lengai. *Journal of Petrology* 37, 1321-1339.
- Biswas, S., Grasemann, B., 2005. Quantitative morphotectonics of the southern Shillong Plateau (Bangladesh/ India). *Australian Journal of Earth Sciences* 97, 82-03.
- Brooker, R.A., 1998. The Effect of CO_2 saturation on Immiscibility between Silicate and Carbonate Liquids: An Experimental Study. *Journal of Petrology* 39, 1905-1915.
- Cabral, R.A., Jackson, M.G., Rose-Koga, E.F., Koga K.T., Whitehouse, M.J., Antonelli, M.A., Farquhar, J., Day, J.M.D., Hauri, E.H., 2013. Anomalous sulphur isotopes in plume lavas reveal deep mantle storage of Archaean crust. *Nature* 496, 490-494.
- Chakmouradian, A.R., 2006. High-field-strength elements in carbonatitic rocks: Geochemistry, crystal chemistry and significance for constraining the sources of carbonatites. *Chemical Geology* 235, 138-160.

- Chaudhuri, S., Ray, J., Koeberl, C., Thöni, M., Dutta, R., Saha, A., Banerjee, M., 2014. Petrology and geochemistry of the ultramafic–mafic Mawpyut complex, Meghalaya: a Sylhet trap differentiation centre in northeastern India. *Geological Journal* 49, 111-128
- Chayes, F., 1949. A simple point counter for thin section. *American Mineralogist* 36, 1-11.
- Chen, W., Simonetti, A., 2013. In-situ determination of major and trace elements in calcite and apatite, and U-Pb ages of apatite from Oka carbonatite complex: insights into a complex crystallization history. *Chemical Geology* 353, 151-172.
- Class, C., Goldstein, S.L., Galer, S.J.G., Weiss, D., 1993. Young formation age of a mantle source. *Nature* 362, 715-721.
- Coffin, M.F., Pringle, M.S., Duncan, R.A., Gladezenko, T.P., Storey, M., Müller, R.D., Gahagan, L.A., 2002. Kerguelen hotspot magma output since 130 Ma. *Journal of Petrology* 43, 1121-1139.
- Courtillot, V., Jacupart, C., Manighetti, I., Tapponnier, P., Besse, J., 1999. On the causal links between flood basalts and continental breakup. *Earth and Planetary Science Letters* 166, 177–195.
- Cox, K.G., Bell, J.D., Pankhurst, R.J., 1979. *The interpretation of igneous rocks*. George Allen & Unwin Publishers Ltd., London, 450p.
- Dalton, J.A., Presnall, D.C., 1998. The continuum of primary-kimberlitic melt composition in equilibrium with lherzolite: data from the system CaO-MgO-Al₂O₃-SiO₂-CO₂ system. *Journal of Petrology* 39, 1953-1964.
- Dai, L. -Q., Zhou, Z.-F., Zheng, Z. -F, 2014. Geochemical insights into the role of metasomatic hornblende in generating alkali basalts. *Geochemistry, Geophysics, Geosystems*, 10.1002/2014GC005486.
- Dawson, J.B., Smith, J.V., Steele, I.M., 1995. Petrology and Mineral Chemistry of Plutonic Igneous Xenoliths from the Carbonatite Volcano, Oldoinyo Lengai, Tanzania. *Journal of Petrology* 36, 797-826.
- Deines, P., 1989. Stable isotopic variation in carbonatites. In: Bell, K. (Ed.), *Carbonatites: Genesis and Evolution*, Unwin Hyman, London, 301-359.
- DePaolo, D.J., 1988. *Neodymium isotope geochemistry: an introduction*. Springer Verlag, New York, p.188.
- Desikachar, S.V., 1974. A review of the tectonic and geological history of eastern India in terms of Plate tectonic theory. *Journal of Geological Society of India* 15, 137-149.
- Dickin, A. P., 1995. *Radiogenic Isotope Geology*. Cambridge University Press, New York, 492p.
- Doroozi, R., Vaccaro, C., Masoudi, F., Petrini, R., 2015. Cretaceous alkaline volcanism in south Marzanabad, northern central Alborz, Iran: Geochemistry and petrogenesis, 1-15.
- Doroshkevich, A. G., Ripp, G. S., Moore, K. R., 2010. Genesis of Khaluta alkaline-basic Ba-Sr carbonatite complex (West Transbaikala, Russia). *Mineralogy and Petrology* 98, 245-268.

- Dosso, L., Bougault, H., Beuzart, P., Calvez, J.Y., Jordan, J.L., 1988. The geochemical structure of the South East Indian Ridge. *Earth and Planetary Science Letters* 88, 47-59.
- Dostal, J., Chatterjee, A. K., 2000. Contrasting behaviour of Nb/Ta and Zr/Hf ratios in a peraluminous granitic pluton (Nova Scotia, Canada). *Chemical Geology* 163, 207-218.
- Downes, H., Balaganskaya, E., Beard, A., Liferovich, R., Demaiffe, D., 2005. Petrogenetic processes in the ultramafic, alkaline and carbonatitic magmatism in the Kola Alkaline Province: A review. *Lithos* 85, 48-75.
- Duncan, R.A., 2002. A time frame for construction of the Kerguelen Plateau and Broken Ridge. *Journal of Petrology* 43, 1109-1119.
- Duncan, R.A., Storey, M., 1992. The life cycle of Indian Ocean hotspots. In: Duncan RA, Rea DK, Kidd RB, Rad U. and Weissel JK (eds.) *Synthesis of results from scientific drilling in the Indian Ocean*, Geophysical Monograph American Geophysical Union 70,91-103.
- Dupuy, C., Michard, A., Dostal, J., Dautel, D., Baragar, W.R.A., 1992. Proterozoic flood basalts from the copper mine river area, northwest territories-isotope and trace-element geochemistry. *Canadian Journal of Earth Sciences* 29, 1934-1943.
- Eby, G. N., 1979. Mount Johnson, Quebec- an example of silicate liquid immiscibility. *Geology* 7, 491-494.
- Eby, G.N., 1975. Abundance and distribution of the rare-earth elements and Yttrium in the rocks and minerals of the Oka carbonatite complex, Quebec. *Geochimica et Cosmochimica Acta* 39, 597-620.
- Evans, P., 1964. The tectonic patterns in northeastern India. *Indian Journal of Earth Science* 107, 103-107.
- Faure, G., 1986. *Principles of isotope geology*. John Wiley and sons, New York, 589p.
- Franz, G., Steiner, G., Volker, F., Pudlo, D., Hammerschmidt, K., 1999. Plume related alkaline magmatism in central Africa-the Meidob Hills (W Sudan). *Chemical Geology* 157, 27-47.
- Freestone, I.C., Hamilton, D.L., 1980. The Role of Liquid Immiscibility in the Genesis of Carbonatites: An Experimental Study. *Contributions to Mineralogy and Petrology* 73, 105-117.
- Frey, F.A., Coffin, M.F., Wallace, P.J., Weiss, D., Zhao, X., Wise, S.W., 2000. Origin and evolution of a submarine large igneous province: the Kerguelen Plateau and Broken Ridge, southern Indian Ocean. *Earth and Planetary Science Letters* 176, 73-89.
- Ghatak, A., Basu, A.R., 2013. Isotopic and trace element geochemistry of alkali-mafic-ultramafic-carbonatitic complexes and flood basalts in NE India: Origin in a heterogeneous Kerguelen plume. *Geochimica et Cosmochimica Acta* 115, 46-72.
- Ghatak, A., Basu, A.R., 2011. Vestiges of the Kerguelen plume in the Sylhet Traps, northeastern India *Earth and Planetary Science Letters* 308, 52-64.
- Gittins, J., 1989. The origin and evolution of carbonatite magma. In: Bell, K. (Ed.), *Carbonatites: Genesis and Evolution*, Unwin Hyman, London, 580-600.

- Gittins, J., Harmer, R.E., 2003. Myth and reality in the carbonatite – silicate rock “association”. *Mineralogy and Petrology* 72, 19-26.
- Goldstein, S.L., O’Nions, R.K., Hamilton, P.J., 1984. A Sm-Nd study of atmospheric dusts and particles from major river systems. *Earth and Planetary Science Letters* 70, 221-236.
- Govindaraju, K., 1994. Compilation of working values and sample description for 383 geostandards. *Geostandards Newsletter -The Journal of Geostandards and Geoanalysis* 18, 1–158.
- Grange, M., Scharer, U., Merle, R., Girardeau, J., Cornen, G., 2010. Plume-Lithosphere interaction during Migration of Cretaceous Alkaline Magmatism in SW Portugal: Evidence from U-Pb ages and Pb-Sr-Hf Isotopes. *Journal of Petrology* 51, 1143-1170.
- Gupta, R.P., Sen, A.K., 1988. Imprints of Ninety- East Ridge in the Shilong Plateau, Indian Shield. *Tectonophysics* 154, 335-341.
- Gwalani, L. G., Rock, N.M.S., Chang, W-J., Fernandez, S., Allegre, C. J., Prinzhofer, A., 1993. Alkaline rocks and carbonatites of Amba Dongar and adjacent areas, Deccan Igneous Province, Gujarat, India. 1. Geology, petrography and petrochemistry. *Mineralogy and Petrology* 47, 219–253.
- Halama, R., Vennemann, T., Siebel, W., Markl, G., 2005. The Grønneidal-Ika Carbonatite-Syenite Complex, South Greenland: Carbonatite formation by Liquid Immiscibility. *Journal of Petrology* 46, 191-217.
- Hamilton, D.L., Bedson, P., Esson, J., 1989. The behavior of trace elements in the evolution of carbonatites. In: Bell, K. (Ed.), *Carbonatites: Genesis and Evolution*, Unwin Hyman, London, pp 405-427.
- Harmer, R., 1999. The Petrogenetic Association of Carbonatite and Alkaline Magmatism: Constraints from the Spitskop Complex, South Africa. *Journal of Petrology* 40, 525-548.
- Harmer, R.E., Gittins, J., 1998. The Case for Primary Mantle derived Carbonatite Magma. *Journal of Petrology* 39, 1895-1903.
- Hart, S.R., Hauri, E.H., Oschmann, L.A., Whitehead, J.A., 1992. Mantle plumes and entrainment: isotopic evidence. *Science* 256, 517-520.
- Hauff, F., Hoernle, K., Tilton, G., Graham, D. W., Kerr, A.C., 2000. Large-volume recycling of oceanic lithosphere over short time scales: Geochemical constraints from the Caribbean large igneous province. *Earth and Planetary Science Letters* 174, 247-263.
- Heaman, L.M., Srivastava, R.K., Sinha, A.K., 2002. A precise U-Pb zircon/baddeleyite age for the Jasra igneous complex, Karbi-Anglong district, Assam, NE India. *Current Science* 82, 744-748.
- Hess, P.C., Rutherford, M.J., 1974. Element fractionation between immiscible melts. *Lunar Science* 5, 328-330.
- Hess, P.C., 1971. Polymer model of silicate melts. *Geochimica et Cosmochimica Acta* 35, 289-306.
- Hirschmann, M.M., Kogiso, T., Baker, M.B., Stolper, E.M., 2003. Alkalic magmas generated by partial melting of garnet pyroxenite. *Geology* 31, 481-484.

- Hirose, K., 1997. Partial melt compositions of carbonated peridotite at 3 GPa and the role of CO₂ in alkali-basalt magma generation. *Geophysical Research Letters* 24, 2837-2840.
- Hofmann, A.W., White, W.M., 1982. Mantle plumes from ancient oceanic crust. *Earth and Planetary Science Letters* 57, 421-436.
- Hoernle, K., Zhang, Y.-S. Graham, D. 1995. Seismic and geochemical evidence for large-scale mantle upwelling beneath the eastern Atlantic and western and central Europe. *Nature* 374, 34-39.
- Hussain, M.F., Ahmad, T., 2009. Geochemical characteristics of the Granitoids of Mikir Hills Massif of Shillong Plateau, Northeast India: Implication for Pan-African Magmatic Activity. *Journal of Virtual Explorer* 32, paper 4.
- Hyndaman, D. W., 1985. *Petrology of igneous and metamorphic rocks*. McGraw-Hill BookCompany, New York, 786p.
- Ingle, S. P., Weiss, D., Scotese, J., Frey, F. A., 2002. Relationship between the early Kerguelen plume and continental flood basalts of the Paleo-Eastern Gondwana margin. *Earth and Planetary Science Letters* 197, 35-50.
- Irvine, T.N., Baragar, W.R.A., 1971. A guide to the chemical classification of the common volcanic rocks. *Canadian Journal of Earth Sciences* 8, 523-548.
- Jacobsen, S.B, Wasserburg, G.J., 1980. Sm-Nd isotopic evolution of chondrites. *Earth and Planetary Science Letters* 50, 139-155.
- Karmalkar, N. R., Duraiswami, R.A., Hoffman, A. 2010. Unusual rift-related carbonatite magmatism from southern Malawi, southeast Africa and its role in crustal evolution. In: Karmalkar NR, Duraiswami RA, Pawar NJ and Sivaji C (eds.) *Origin and evolution of the deep continental crust*, Narosa Publishers, New Delhi, 153-172.
- Kayal, J.R., Arefiev, S.S., Barua, S., Hazarika, D., Gogoi, N., Kumar, A., Chowdhury, S.N., Kalita, S., 2006. Shillong Plateau earthquake in northeast India region: Complex tectonic model. *Current Science* 91, 109–114.
- Kent, R.W., Pringle, M.S., Müller, R.D., Saunders, A.D., Ghose, N.C., 2002. ⁴⁰Ar/³⁹Ar geochronology of the Rajmahal basalts, India, and their relationship to the Kerguelen Plateau. *Journal of Petrology* 43, 1141-1153.
- Kjarsgaard, B.A., Hamilton, D.L., 1988. Liquid Immiscibility and the origin of Alkali-Poor Carbonatites. *Mineralogical Magazine* 52, 43-55.
- Koeberl, C., 1993. Instrumental neutron activation analysis of geochemical and cos-mochemical samples: a fast and reliable method for small sample analysis. *Journal of Radio-analytical and Nuclear Chemistry* 168, 47-60.
- Kürkcüoğlu, B., 2010. Geochemistry and Petrogenesis of basaltic rocks from the Develidağ volcanic complex, Central Anatolia, Turkey. *Journal of Asian Earth Sciences* 37, 42-51.
- Larsen, L.M., 1976. Clinopyroxenes and Coexisting Mafic Minerals from the Alkaline Ilímaussaq Intrusion, South Greenland. *Journal of Petrology* 17, 258-290.

- Lassiter, J.C., DePaolo, J., 1997. Plume/lithosphere interaction in the generation of continental and oceanic flood basalts: chemical and isotopic constraints. *Geophysical Monograph* 100, 335-355.
- Le Bas, M. J., 1989. Diversification of carbonatite. In: Bell, K. (Ed.), *Carbonatites: Genesis and Evolution*, Unwin Hyman, London, 428-447.
- Le Bas, M.J., 1987. Nephelinites and Carbonatites. In: Fitton, J.G., Upton, U.B.J. (Eds.), *Alkaline Igneous Rocks*, Geological Society of London Special Publication 30, 85-94.
- Ma, G.S.-K, Malpas, J., Xenophontos, C., Chan, G. H.-N., 2011. Petrogenesis of Latest Miocene-Quaternary Continental Intraplate Volcanism along the Northern Dead Sea Fault System (Al Ghab-Homs Volcanic Field), Western Syria: Evidence for Lithosphere-Asthenosphere Interaction. *Journal of Petrology* 52, 401-430.
- Macdonald, R., Kjarsgaard, B.A., Skilling, I.P., Davies, G.R., Hamilton, D.L., Black, S., 1993. Liquid immiscibility between trachyte and carbonate in ash flow tuffs from Kenya. *Contributions to Mineralogy and Petrology* 114, 276-287.
- Mader, D., Koeberl, C., 2009. Using Instrumental Neutron Activation Analysis for geochemical analyses of terrestrial impact structures: Current analytical procedures at the University of Vienna Geochemistry Activation Analysis Laboratory. *Applied Radiation and Isotopes* 67, 2100-2103.
- Mahoney, J.J., Jones, W.B., Frey, F.A., Salters, V.J.M., Pyle, D.G., Davies, H.L., 1995. Geochemical characteristics of lavas from Broken Ridge, the Naturaliste Plateau and southernmost Kerguelen Plateau: Cretaceous plateau volcanism in the southeast Indian Ocean. *Chemical Geology* 120, 315-345.
- Mahoney, J.J., Roex, A.P., Peng, Z., Fisher, R.L., Natland, J.H., 1992. Southwestern limits of Indian Ocean Ridge mantle and the origin of low $^{206}\text{Pb}/^{204}\text{Pb}$ mid-ocean ridge basalt: Isotope systematics of the Central Southwest Indian Ridge (17° - 50° E). *Journal of Geophysical Research* 97, 19771-19790.
- Mahoney, J.J., Macdougall, J.D., Lugmair, G.W., Gopalan, K., 1983. Kerguelen hotspot source for Rajmahal Traps and Ninetyeast Ridge? *Nature* 303, 385-389.
- Majumdar, D., 2010. Need to intensify base metal exploration activities in Mikir Hills, northeastern India. *Current Science* 99(5), 656-662.
- Martins, S., Mata, J., Munhá, J., Mendes, M.H., Maerschalk, C., Caldeira, R., Mattielli, N., 2010. Chemical and mineralogical evidence of the occurrence of mantle metasomatism by carbonate-rich melts in an oceanic environment (Santiago Island, Cape Verde). *Mineralogy and Petrology* 99, 43-65.
- Marzoli, A., Piccirillo, E.M., Renne, P.R., Bellieni, G., Iacumin, M., Nyobe, J.B., Tongwa At., 2000. The Cameroon Volcanic Line Revisited: Petrogenesis of Continental Basaltic Magmas from Lithospheric and Asthenospheric Mantle Sources. *Journal of Petrology* 41, 87-109.
- Mazumder, S.K., 1976. A summary of the Precambrian geology of the Khasi hills, Meghalaya. *Geological Survey of India Miscellaneous Publication* 23, 311-334.

- McDonald, G.A., Katsura, T., 1964. Chemical composition of Hawaiian lavas. *Journal of Petrology* 5, 82-113.
- McKenzie, D., Onions, R.K., 1995, The source regions of ocean island basalts: *Journal of Petrology* 36, 133–159.
- Melluso L., Srivastava R.K., Guarino, V., Zanetti, A., Sinha, A.K., 2010. Mineral compositions and petrogenetic evolution of the Ultramafic-Alkaline-Carbonatite complex of Sung Valley, Northeastern India. *Canadian Mineralogist* 48, 205–229.
- Melluso, L., Srivastava, R. K., Petrone, C. M., Guarino, V. and Sinha, A. K., 2012. Mineralogy, magmatic affinity and evolution of the Early Cretaceous alkaline complex of Jasra, Shillong Plateau, northeastern India. *Mineralogical Magazine* 76, 1099-1117
- Michard, A., Montigny, R., Schlich, R., 1986. Geochemistry of the mantle beneath the Rodriguez triple junction and the South-East Indian Ridge. *Earth and Planetary Science Letters* 78, 104-114.
- Mitchell, R.H., 2005. Carbonatites and Carbonatites and Carbonatites. *Canadian Mineralogist* 43, 2049-2068.
- Mukhopadhyay, S., Ray, J., Balaram, V., Krishna, A. K., Ghosh, B., Mukhopadhyay, S., 2011. Geochemistry and petrogenesis of syenites and associated rocks of the Elagiri complex, Southern Granulite Terrane, India. *Journal of Asian Earth Sciences* 42, 1256-1270.
- Muller, R.D., Royer, J. Y., Lawyer, L.A., 1993. Revised plate motions relative to the hot spots from combined Atlantic and Indian Ocean hotspot tracks. *Geology* 16, 275-278.
- Nag, S., Sengupta, S.K., Gaur, R.K., Absar, A., 1999. Alkaline rocks of Samchampi-Samteran, District Karbi Anglong, Assam, India. *Journal of Earth System Science* 108, 33-48.
- Nakata, T., 1989. Active faults of the Himalaya of India and Nepal. In: Malinconica, L.L., Jr. Lillie, R.L. (Eds.), *Tectonics of the Western Himalayas*. Geological Society of America Special Paper 232, 243–264.
- Nandy, D.R., 2001. *Geodynamics of North Eastern India and the adjoining region*. acb Publication, Calcutta, p. 120.
- Nandy, D.R., 1980. Tectonic patterns in northeastern India. *Indian Journal of Earth Science* 7, 103-107.
- Nelson, D.R., Chivas, A.R., Chappell, B.W., McCulloch, M.T., 1988. Geochemical and isotopic systematics in carbonatites and implications for the evolution of ocean island sources. *Geochimica et Cosmochimica Acta* 52, 1-17.
- Nicolaysen, K., Bowring, S., Frey, F., Weiss, D., Ingle, S., Pringle, M.S., Coffin, M.F., 2001. Provenance of Proterozoic garnet-biotite gneiss recovered from Elan Bank, Kerguelen Plateau, southern Indian Ocean. *Geology* 29, 235-238.
- Petibon, C.M., Jenner, G.A., Kjarsgaard, B.A., 1998. The genesis of natrocarbonatites: constraints from experimental petrology and trace element partition coefficients. *Mineralogical Magazine* 62A, 1161-1162.

- Philpotts, A. R., 1982. Composition of immiscible liquids in volcanic rocks. *Contributions to Mineralogy and Petrology* 80, 201–218.
- Pilet, S., Baker, M.B., Müntener, O., Stolper, E.M., 2011. Monte Carlo Simulations of Metasomatic Enrichment in the Lithosphere and Implications for the Source of Alkaline Basalts. *Journal of Petrology* 52, 1415-1442.
- Pilet, S., Ulmer, P., Villiger, S., 2010. Liquid line of descent of a basanitic liquid at 1.5 GPa: constraints on the formation of metasomatic veins. *Contributions to Mineralogy and Petrology* 159, 621-643.
- Pilet, S., Baker, M.B., Stolper, E.M., 2008. Metasomatized lithosphere and the origin of alkaline lavas. *Science* 320, 916-919.
- Pilet, S., Hernandez, J., Sylvester, P., Poujol, M., 2005. The metasomatic alternative for ocean island basalt chemical heterogeneity. *Earth and Planetary Science Letters* 236, 148-166.
- Pirajno, F., Ernst, R.E., Borisenko, A.S., Fedoseev, G., Naumov, E.A., 2009. Intraplate magmatism in central Asia and China and associate metallogeny. *Ore Geology Reviews* 35, 114-136.
- Poletti, J.A., Cottle, J.M., Hagen-Peter, G.A., Lackey, J.S., 2016. Petrochronological Constraints on the Origin of the Mountain Pass Ultrapotassic and Carbonatite Intrusive Suite, California. *Journal of Petrology* 57 (8), 1555-1598.
- Rajesh, H. M., 2003. Outcrop-scale silicate liquid immiscibility from an alkali syenite (A-type granitoid)-pyroxenite association near Puttetti, Trivandrum Block, South India. *Contributions to Mineralogy and Petrology* 145, 612-627.
- Ray J., Saha A., Koeberl C., Thoni M., Ganguly S., Hazra S., 2013. Geochemistry and Petrogenesis of Proterozoic mafic rocks from East Khasi Hills, Shillong Plateau, Northeastern India. *Precambrian Research* 230, 119-137.
- Ray, J.S., 2009. Radiogenic Isotopic Ratio Variations in Carbonatites and Associated Alkaline Silicate Rocks: Role of Crustal Assimilation. *Journal of Petrology* 50, 1955-1971.
- Ray, J.S., Pattanayak, S.K., Pande, K., 2005. Rapid emplacement of the Kerguelen plume-related Sylhet Traps, eastern India: Evidence from $^{49}\text{Ar}/^{39}\text{Ar}$ geochronology. *Geophysical Research Letters* 32, 1-4.
- Ray, J.S., Pande, K., 2001. ^{40}Ar - ^{39}Ar age of carbonatite-alkaline magmatism in Sung Valley, Meghalaya, India. *Journal of Earth System Sciences* 110, 185-190.
- Ray, J.S., Trivedi, J.R., Dayal, A.M., 2000. Strontium isotope systematics of Amba Dongar and Sung Valley carbonatite-alkaline complexes, India: evidence for liquid immiscibility, crustal contamination and long-lived Rb/Sr enriched mantle sources. *Journal of Asian Earth Sciences* 18, 585-594.
- Ray, J.S., Ramesh, R., Pande, K., 1999. Carbon isotopes in Kerguelen plume-derived carbonatites: evidence for recycled inorganic carbon. *Earth and Planetary Science Letters* 170, 205-214.
- Roedder, E., 1951. Low temperature liquid immiscibility in the system K_2O - FeO - Al_2O_3 - SiO_2 . *American Mineralogist* 36, 282-286.

- Rudnick, R.L., McDonough, W.F., Chappell, B.W., 1993. Carbonatite metasomatism in the northern Tanzanian mantle-petrographic and geochemical characteristics. *Earth and Planetary Science Letters* 114, 463-475.
- Safonova, I.Y., 2009. Intraplate magmatism and oceanic plate stratigraphy of the Paleo-Asian and Paleo-Pacific Oceans from 600 to 140 Ma. *Ore Geology Reviews* 35, 137-154.
- Safonova, I., Maruyama, S., 2013. Asia: a frontier of a future supercontinent. In: Kim, S.W., Park, S., (Eds.), 2013 IAGR Annual Convention and 10th International Symposium on Gondwana to Asia, September 30-October 4, 2013, Daejeon, Korea. IAGR Conference Series, No. 4, 20-22.
- Safonova, I.Y., Simonov, V.A., Buslov, M.M., Ota, T., Maruyama, S., 2008. Neoproterozoic basalts of the Paleo-Asian Ocean (Kurai accretionary zone, Gorny Altai, Russia): geochemistry, petrogenesis and geodynamics. *Russian Geology and Geophysics* 49, 254-271.
- Saha, A., Ray, J., Ganguly, S., Chatterjee, N., 2011. Occurrence of melanite garnet in syenite and ijolite-melteigite rocks of Samchampi-Samteran alkaline complex, Mikir Hills, Northeastern India. *Current Science* 101, 95-100.
- Saha, A., Ganguly, S., Ray, J., Chatterjee, N., 2010a. Evaluation of phase chemistry and petrochemical aspects of Samchampi-Samteran differentiated alkaline complex of Mikir Hills, Northeastern India. *Journal of Earth System Science* 119, 675-699.
- Saha, A., Ganguly, S., Ray, J., Dhang, A., 2010b. Vanadium bearing titaniferous magnetite ore bodies of Ganjang, Karbi- Anglong district, NE India. *Journal of Geological Society of India* 76, 26-32.
- Santosh, M., Maruyama, S., Komiya, T., Yamamoto, S., 2010. Orogens in the evolving earth: from surface continents to 'lost continents' at the core-mantle boundary. In: Kusky, T., Zhai, M.-G., Xiao, W., (Eds.), *The Evolving Continents: Understanding Processes of Continental Growth*. Geological Society of London Special Publications 338, 77-116.
- Schultz, F., Lehmann, B., Tawackoli, S., Rössling, R., Belyatsky, B., Dulski, P., 2004. Carbonatite diversity in the Central Andes: the Ayopaya alkaline province, Bolivia. *Contributions to Mineralogy and Petrology* 148, 391-408.
- Segev, A., 2002. Flood basalts, continental breakup and dispersal of Gondwana: evidence for periodic migration of upwelling mantle flows (plumes). *EGU Stephan Muller Special Publication Series* 2, 171-191.
- Sen, G., 1995. A simple petrological model for the generation of Deccan Trap Magmas. *International Geology Reviews* 37, 825-850.
- Sensarma, S., Palme, H., 2013. Silicate liquid immiscibility in the ~2.5 Ga Fe-rich andesite at the top of the Dongargarh large igneous province (India). *Lithos* 170-171, 239-251.
- Simonetti, A., Bell, K., 1994. Isotopic and geochemical investigation of Chilwa Island Carbonatite complex, Malwai: evidence for a depleted mantle source region, liquid immiscibility, and open system behaviour. *Journal of Petrology* 35, 1547-1621.

- Simonov, V.A., Mikolaichuk, A.V., Safonova, I. Yu, Kotlyarov, A.V., Kovyazin, S.V., 2015. Late Paleozoic–Cenozoic intra-plate continental basaltic magmatism of the Tianshan–Junggar region in the SW Central Asian Orogenic Belt. *Gondwana Research* 27, 1646-1666.
- Sleep, N.H., 2006. Mantle plumes from top to bottom. *Earth Science Review* 77, 231-271.
- Son, T.H., Koeberl, C., 2005. Chemical variation within fragments of Australasian tektites. *Meteorite Planetary Science* 40, 805-815.
- Song, X-Y., Qi, H-W., Robinson, P.T., Zhou, M-F., Cao, Z-M., Chen, L-M., 2008. Melting of the subcontinental lithospheric mantle by the Emeishan mantle plume; evidence from the basal alkaline basalts in Dongchuan, Yunan, Southwestern China. *Lithos* 100, 93-111.
- Srivastava, R. K., Sinha, A. K., 2007. Petrogenesis of the Early Cretaceous Ultramafic–Mafic–Alkaline–Carbonatite Igneous complexes from the Shillong Plateau, NE India. In: Ray, J., Bhattacharyya, C. (Eds.), *Igneous Petrology: 21st century perspective*, Allied Publishers, New Delhi, 143-164.
- Srivastava, R.K., Sinha, A.K., 2004a. Geochemistry of Early Cretaceous alkaline ultramafic-mafic complex from Jasra, Karbi Anglong, and Shillong Plateau, northeastern India. *Gondwana Research* 7, 549–561.
- Srivastava, R.K., Sinha, A.K., 2004b. Early Cretaceous Sung Valley ultramafic-alkaline-carbonatite complex, Shillong Plateau, northeastern India: Petrological and genetic significance. *Mineralogy and Petrology* 80, 241–263.
- Srivastava, R.K., Taylor, A., 1996. Carbon-Oxygen-Isotopes variation in Indian carbonatites. *International Geological Review* 38, 419-429.
- Srivastava, R.K., Heaman, L.M., Sinha, A.K., Shihua, S., 2005. Emplacement age and isotope geochemistry of Sung Valley alkaline-carbonatite complex, Shillong Plateau, northeastern India: Implications for primary carbonate melt and genesis of the associated silicate rocks. *Lithos* 81, 33-54.
- Srivastava, R.K., Melluso, L., Sinha, A.K., 2016. Petrogenesis of an early Cretaceous potassic lamprophyre dyke from Rongjeng, East Garo Hills, Shillong plateau, north-eastern India. *Current Science* 110, 649-658.
- Storey, M., Kent, R.W., Saunders, A.D., Hergt, J., Salters, V.J.M., Whitechurch, H., Sevigny, J.H., Thirlwall, M.F., Leat, P., Ghose, N.C., Grifford, M., 1992. Lower Cretaceous volcanic rocks on continental margins and their relationship to the Kerguelen Plateau. *Proceedings Ocean Drilling Program Scientific Results* 120, 33-53.
- Subrahmanyam, N. P., Leelanandam, C., 1989. Differentiation due to probable initial immiscibility in the Musala Pluton of the Mundwara Alkali Igneous Complex, Rajasthan, India. In: Leelanandam, C.(Ed.), *Alkaline rocks*, Geological Society of India Memoir 15, 25-46.
- Sun, S.S., McDonough, W.F., 1989. Chemical and isotopic systematics of oceanic basalts: implications for mantle composition and processes. In: Saunders, A.D., Norry, M.J. (Eds.), *Magmatism in the ocean basins*, Geological Society of London Special Publication 42, 313-345.

- Toyoda, K., Horiuchi, H., Tokonami, M., 1994. Dupal anomaly of Brazilian carbonatites: geochemical correlation with hotspots in the South Atlantic and implications for the mantle source. *Earth and Planetary Science Letters* 126, 315-331.
- Veena, K., Pandey, B.K., Krishnamurthy, P., Gupta, J.N., 1998. Pb, Sr and Nd isotopic systematics of the carbonatites of the Sung Valley, Meghalaya, northeast India: implications for contemporary plume-related mantle source characteristics. *Journal of Petrology* 39, 1875-1884.
- Veksler, I.V., Nielsen, T.F., Sokolov, S.V., 1998. Mineralogy of crystallized melt inclusions from Gardiner and Kovdor Ultramafic Alkaline Complexes: Implications for Carbonatite Genesis. *Journal of Petrology* 39, 2015-2031.
- Verhulst, A., Balaganskaya, E., Kirnarsky, Y., Demaiffe, D., 2000. Petrological and geochemical (trace elements and Sr-Nd isotopes) characteristics of the Paleozoic Kovdor ultramafic, alkaline and carbonatite intrusion (Kola Peninsula, NW Russia). *Lithos* 51, 1-25.
- Visser, W., Koster van Groos, A. F., 1979. Phase relations in the system $K_2O-FeO-Al_2O_3-SiO_2$ at 1 atmosphere with special emphasis on low temperature liquid immiscibility. *American Journal of Science* 279, 70-91.
- Watson, E.B., 1976. Two liquid partition coefficients: Experimental data and geochemical implications. *Contributions to Mineralogy and Petrology* 56, 119-134.
- Warner, R.D., 1973. Liquidus relations in the system $CaO-MgO-SiO_2-H_2O$ at 10 PH₂O and their petrologic significance. *American Journal of Science* 273, 925-946.
- Weaver, B.L., 1991. The origin of ocean island basalt end member compositions: trace element and isotopic constraints. *Earth and Planetary Science Letters* 104, 381-397.
- White, W.M., 2010. Oceanic Island Basalts and Mantle Plumes: The Geochemical Perspective. *Annual Review of Earth and Planetary Science* 38, 133-160.
- Wilson, M., 1989. *Igneous Petrogenesis*, Unwin Hyman, London, 466p.
- Woolley, A.R., Kempe, D.R.C., 1989. Carbonatite: Nomenclature, average chemical compositions and element distribution. In: Bell, K. (Ed.), *Carbonatites: Genesis and Evolution*. Unwin Hyman, London, 1-14.
- Wyllie, P., Barker, M. B., White, B., 1990. Experimental boundaries for the origin and evolution of carbonatites. *Lithos* 26, 3-9.
- Wyllie, P.J., Huang, W.I., 1976. Carbonation and melting reactions in the system $CaO-MgO-SiO_2-CO_2$ at mantle pressures with geophysical and petrological applications. *Contributions to Mineralogy and Petrology* 54, 79-107.
- Yin, An., Dubey, C.S., Webb, A.A.G., Kelty, T.K., Grove, M., Gehrels, G.E., Burgess, W.P., 2010. Geologic correlation of the Himalayan orogen and Indian craton: Part 1. Structural geology, U-Pb zircon geochronology, and tectonic evolution of the Shillong Plateau and its neighboring regions in NE India. *Bulletin Geological Society of America* 122, 336-359.
- Zindler, A., Hart, S.R., 1986. Chemical geodynamics. *Annual Review Earth and Planetary Sciences* 14, 493-571.

Figure Caption

Fig.1: Regional geological and tectonic framework of the Shillong Plateau (Srivastava and Sinha, 2004a; 2004b)

Fig.2: Geological map of Samchampi-Samteran ultramafic-mafic-alkaline-carbonatite complex (Saha et al., 2010a; 2010b). Inset map shows map shows location of study area in the map of India

Fig.3:(A) Photomicrograph of syenite from SSAC showing an overall hypidiomorphic granular texture marked by K-feldspar, clinopyroxene and plagioclase.

(B) Photomicrograph depicting hypidiomorphic granular texture in melteigite (in between cross polars). The textural pattern is defined by clinopyroxene (Cpx), biotite (B) and nepheline (N)

(C) Photomicrograph showing cumulus texture in alkali pyroxenite (in between cross polars). Clinopyroxene (Cpx) grains represent the cumulus phase while nepheline (N) represent the intercumulus phase

(D) Photomicrograph showing overall poikilitic relationship between clinopyroxene (Cpx) and K-feldspar (K) in shonkinite (in between cross polars)

(E) Photomicrograph showing fractured nepheline(N) grain, in nepheline syenite, poikilitically enclosing clinopyroxene (Cpx) grains (in between cross polars)

(F) Photomicrograph depicting hypidiomorphic granular texture in carbonatite with stubby apatite (Ap) grains randomly scattered within calcite(C) defining a mosaic pattern (in between cross polars)

Fig.4: Plots showing variations of major oxides (wt.%) against SiO₂ for Samchampi-Samteran alkaline rocks

Fig.5:

(A) Plots of alkaline silicate rocks from SSAC in Total alkali-silica (TAS) diagram (after Cox et al., 1979) adapted by Wilson (1989) for plutonic igneous rocks. The curved solid line (after Irvine and Baragar, 1971) subdivides the alkaline from subalkaline rocks.

(B) Compositional plots of alkaline silicate rocks from Samchampi-Samteran complex in Total alkali-silica (TAS) diagram. The curved solid line (after McDonald and Katsura, 1964) subdivides the alkaline from subalkaline rocks

(C) Plots of alkaline silicate rocks from Samchampi-Samteran complex in Total alkali-silica (TAS) diagram. Field boundaries are after Hyndaman (1985)

Fig.6: Plots showing variations of trace elements against SiO₂ for Samchampi-Samteran alkaline rocks

Fig.7: Chondrite normalized rare earth element and Primitive mantle normalized incompatible trace element patterns for alkaline-carbonatite rocks of Samchampi-Samteran. Normalization factors after Sun and McDonough (1989)

Fig.8: Plots of Samchampi-Samteran alkaline silicates and carbonatites in Ba/La vs. mg no. diagram

Fig.9:

- (A) Plot of Samchampi-Samteran samples in ϵ_{Nd} vs. $^{87}Sr/^{86}Sr$ isotope correlation diagram showing their relationship with different lithologies from Mawpyut (Chaudhuri et al., 2013), Jasra (Srivastava and Sinha, 2004a), Sung Valley (Srivastava et al., 2005) complexes and Kerguelen Plateau Basalts. The array of plots reflects an EMII (enriched mantle II) signature. Fields of various Oceanic Plateau Basalts are after Hauff et al. (2000)
- (B) $^{143}Nd/^{144}Nd_{initial}$ vs. $^{87}Sr/^{86}Sr_{initial}$ isotope correlation plot for Samchampi-Samteran samples. Main oceanic mantle components after Zindler and Hart (1986) are shown. The mantle array is defined by many oceanic basalts and bulk earth values of $^{143}Nd/^{144}Nd$ and $^{87}Sr/^{86}Sr$ can be observed from this trend (Faure, 1986; Dickin, 1995). The field for Kerguelen Plateau Basalt is based on Michard et al. (1986), Dosso et al. (1988), Storey et al. (1992) and Mahoney et al. (1995)

Fig.10: ϵ_{Nd} vs. $^{87}Sr/^{86}Sr_{initial}$ diagram for Samchampi-Samteran samples of present study with plots of different lithologies from Mawpyut (Chaudhuri et al., 2014), Jasra (Srivastava and Sinha, 2004a) and Sung Valley (Srivastava et al., 2005) complexes. Fields of SEIR, MORB, Rajmahal tholeiites, Shylhet Trap basalts from CH (Cherrapunji) and MB (Mawsinram-Baylot) section and Kerguelen Plateau Basalts are after Michard et al. (1986), Dosso et al. (1988), Storey et al. (1992), Mahoney et al. (1995), Ghatak and Basu (2011)

Fig.11: A schematic model showing the tectonic evolution of Samchampi-Samteran alkaline complex (SSAC) (based on Pirajno et al, 2009; Santosh et al., 2010, Safonova and Maruyama, 2013 and Simonov et al., 2015).

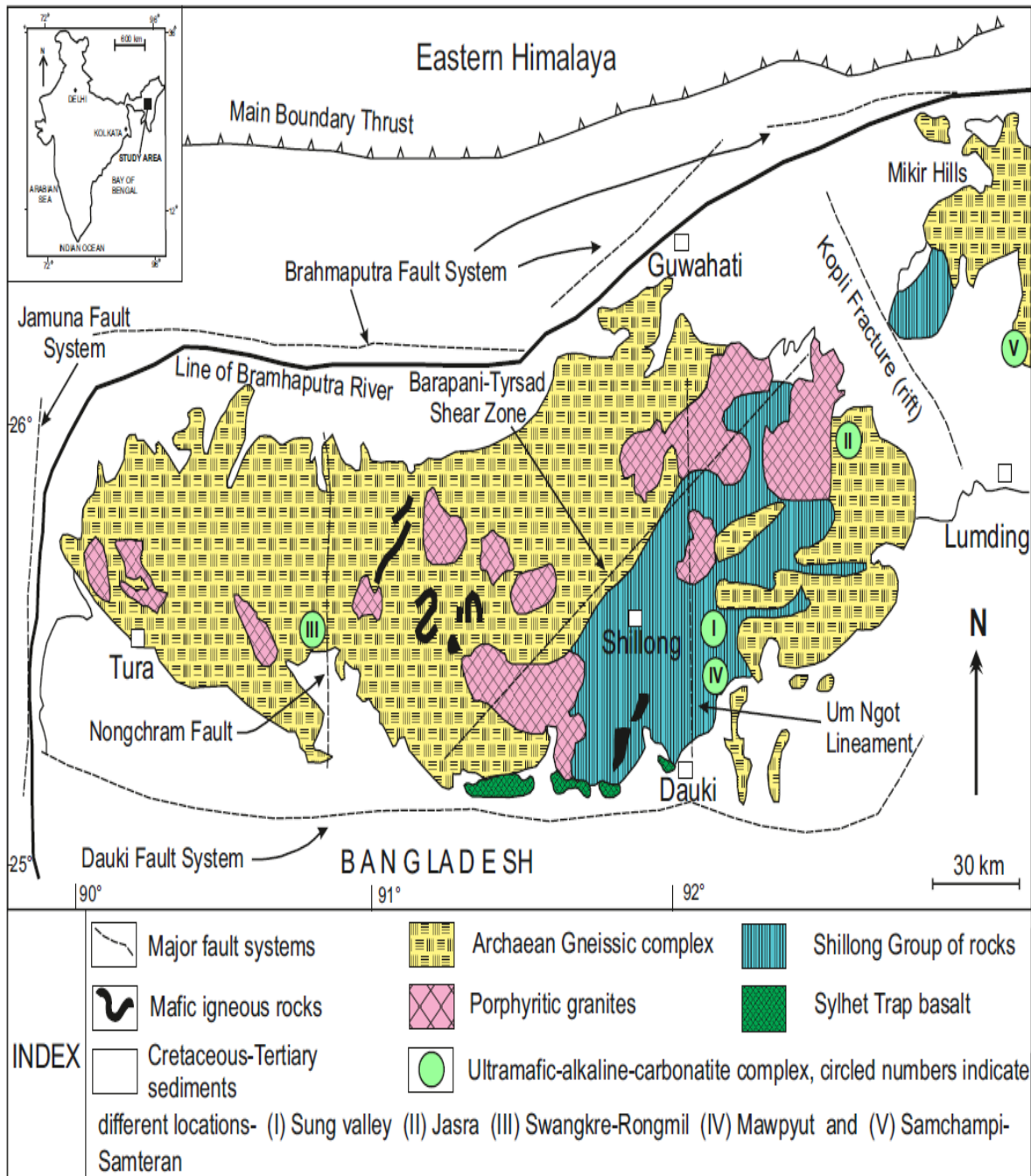


Fig. 1

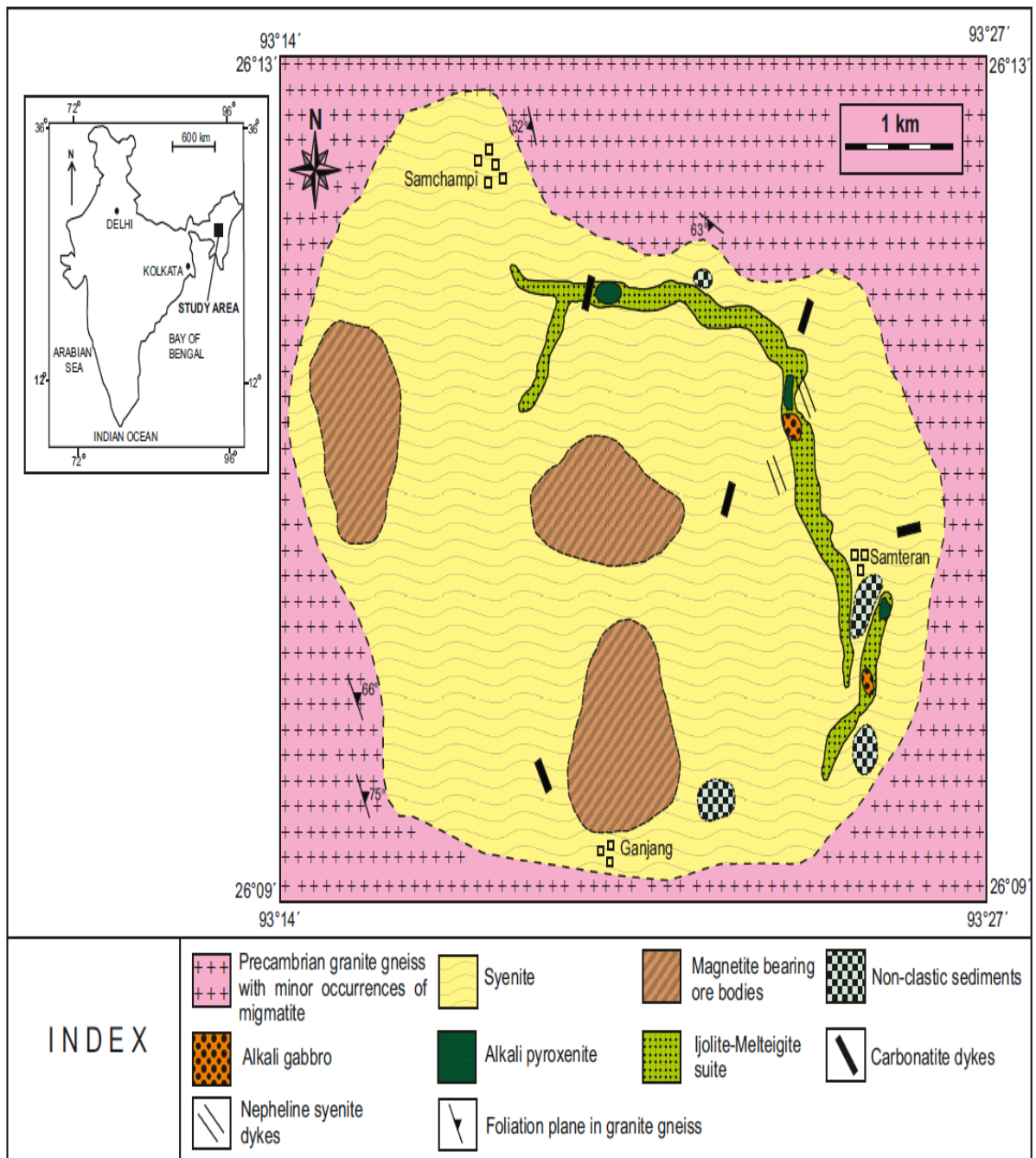


Fig. 2

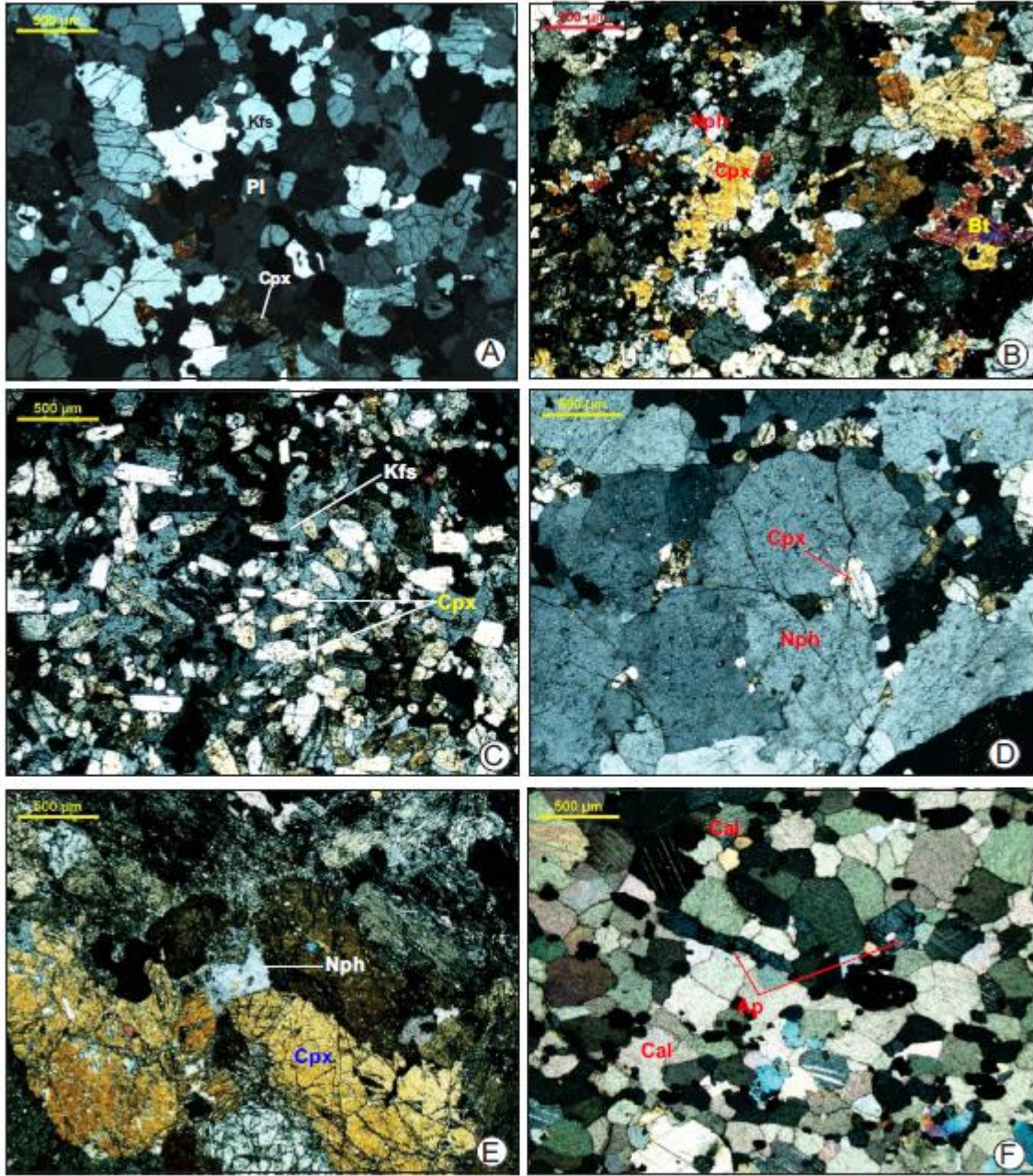


Fig. 3

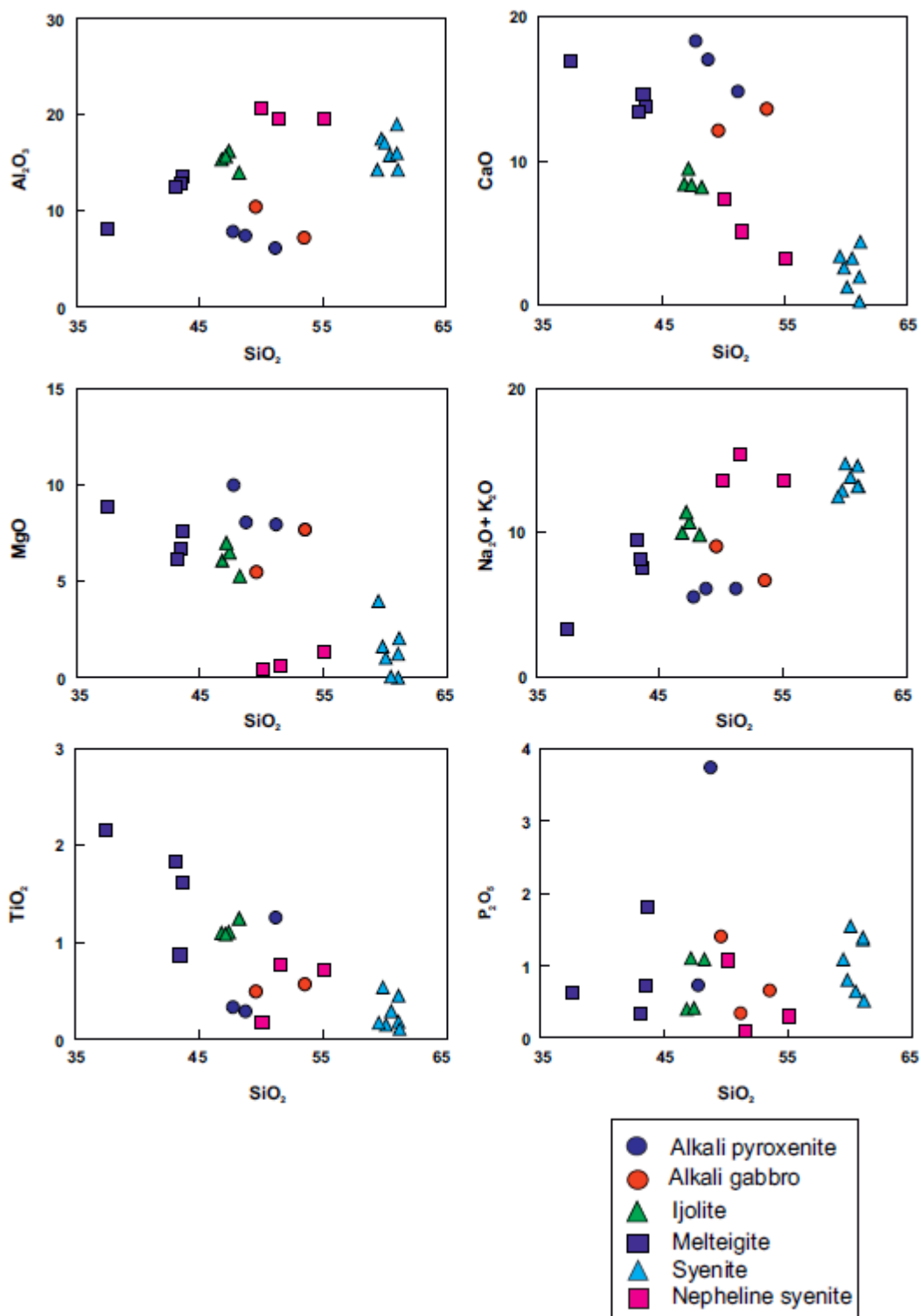


Fig.4

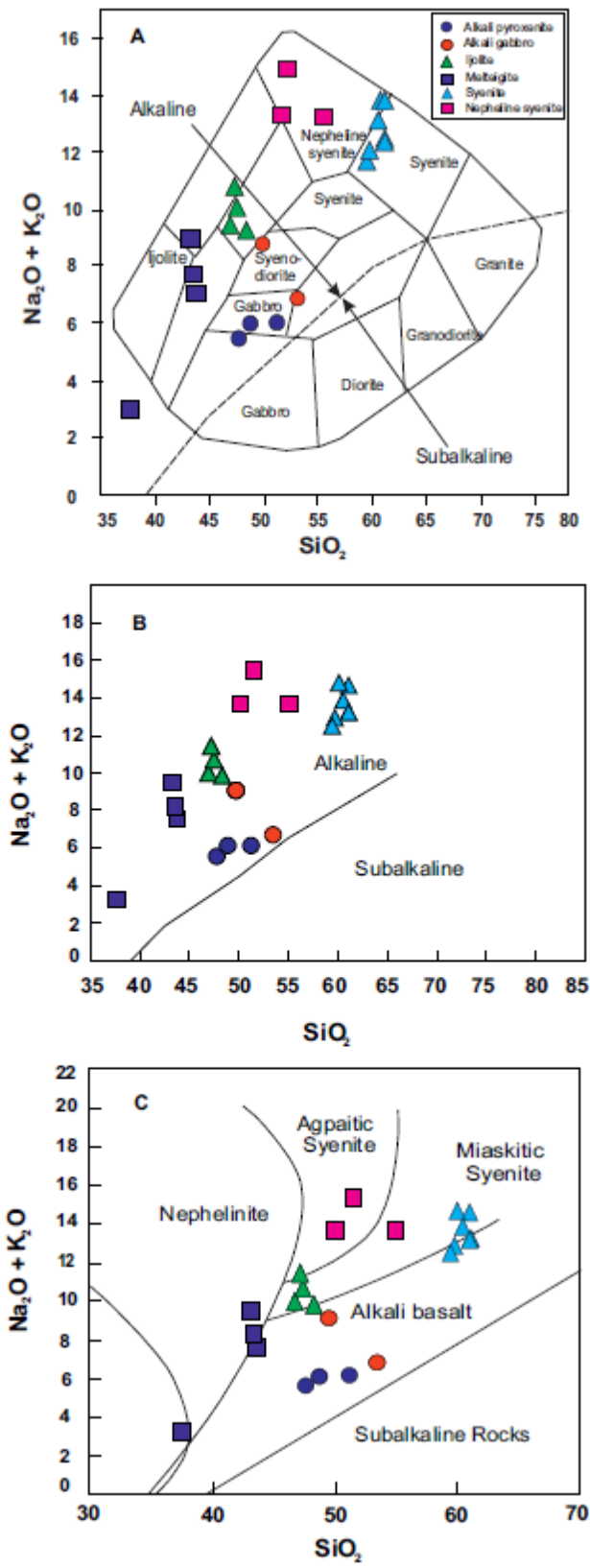


Fig.5

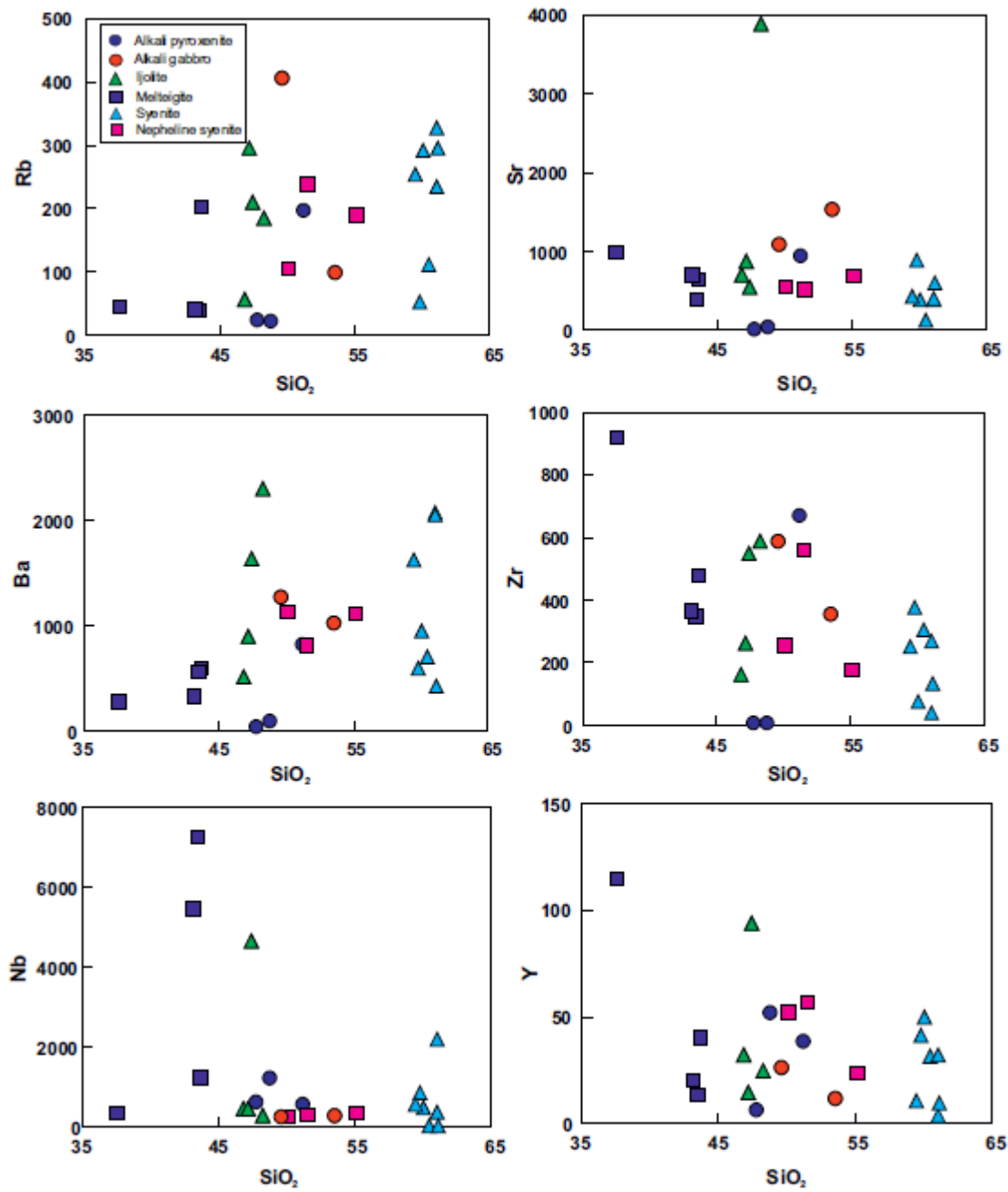


Fig.6

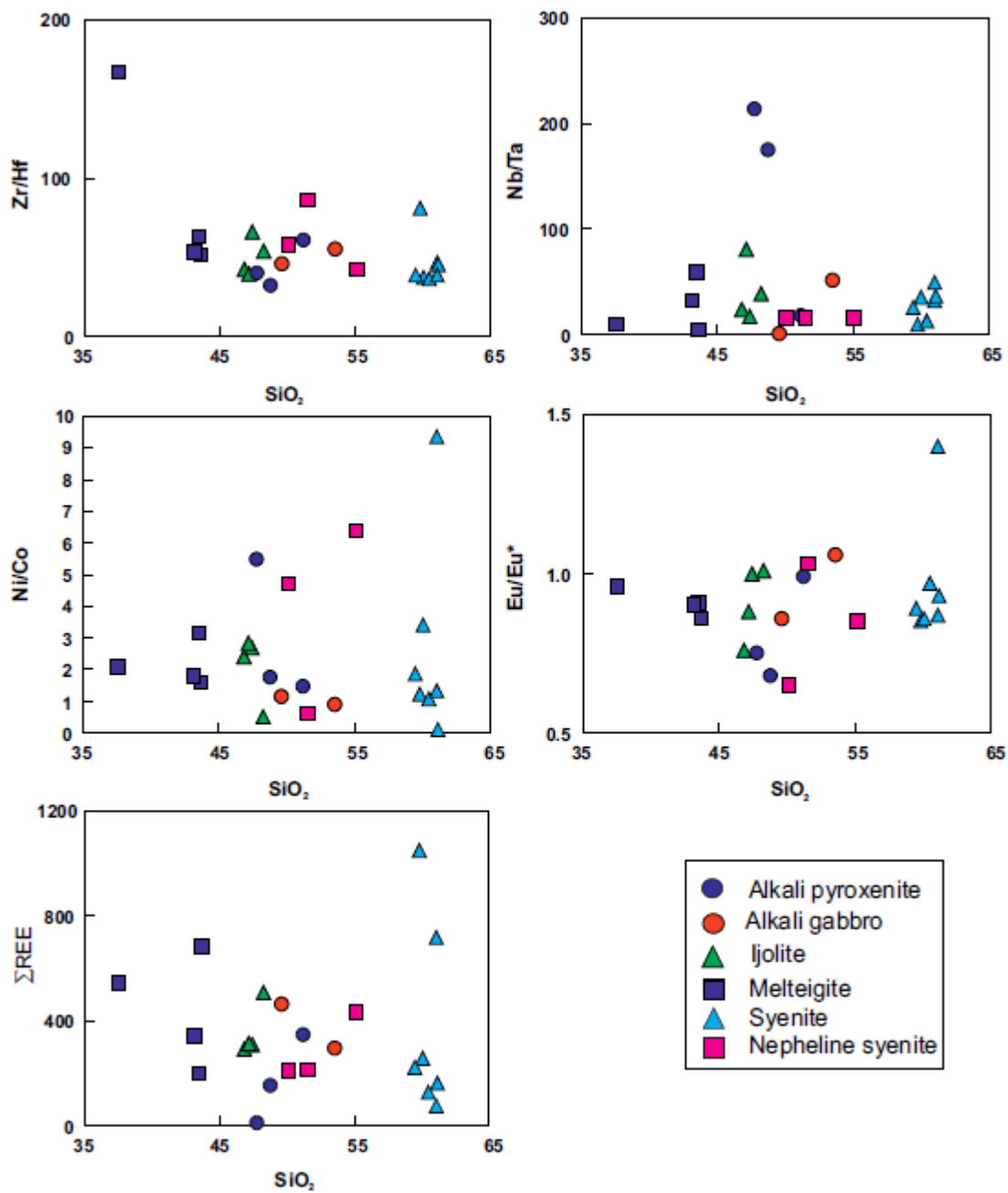


Fig. 6 Contd...

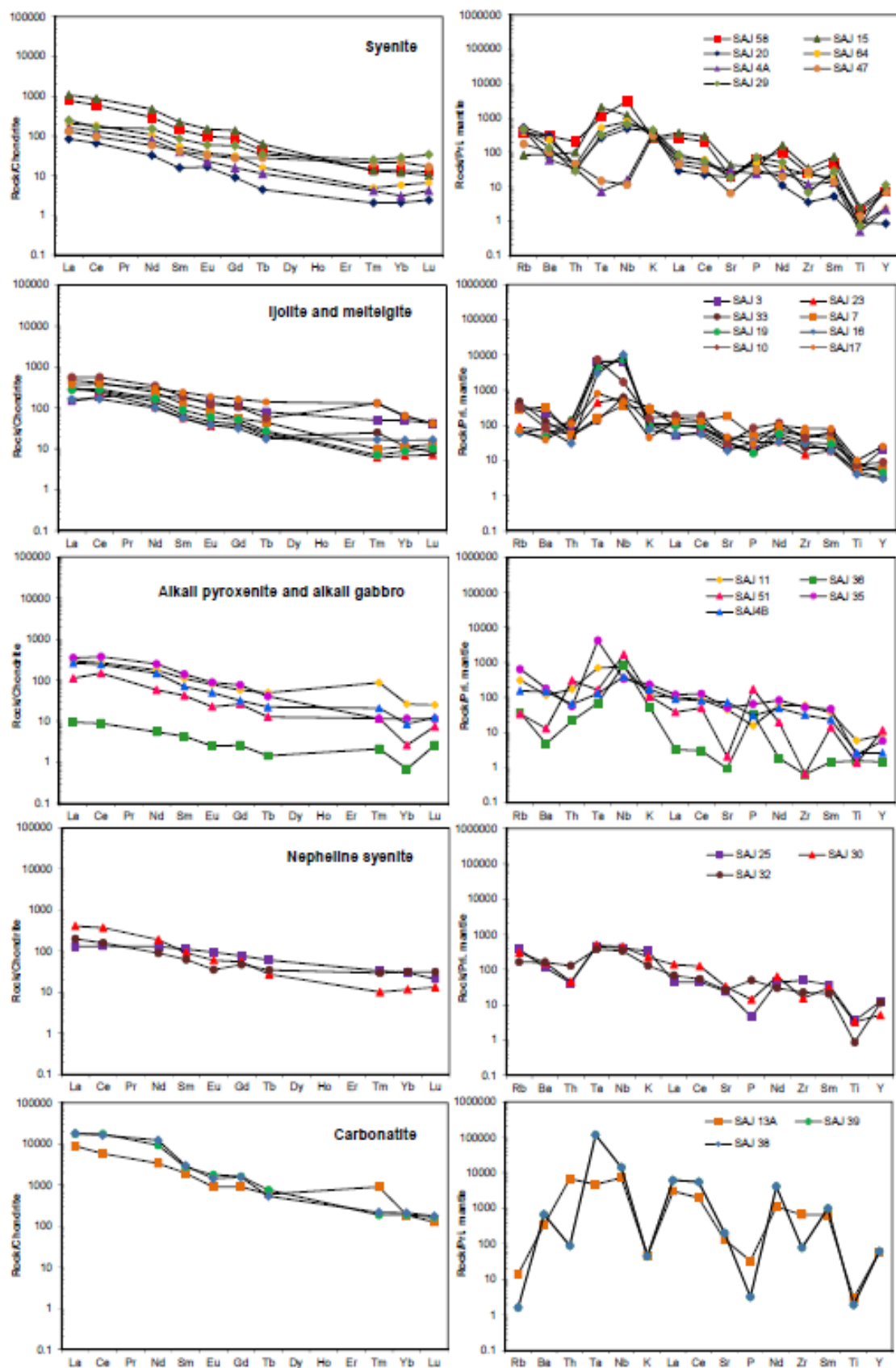


Fig. 7

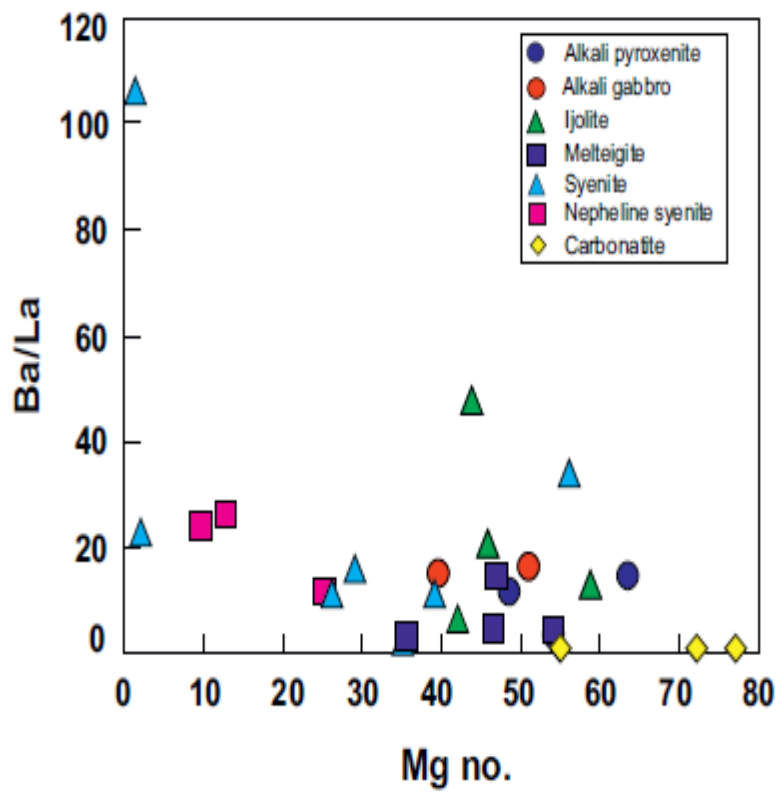


Fig. 8

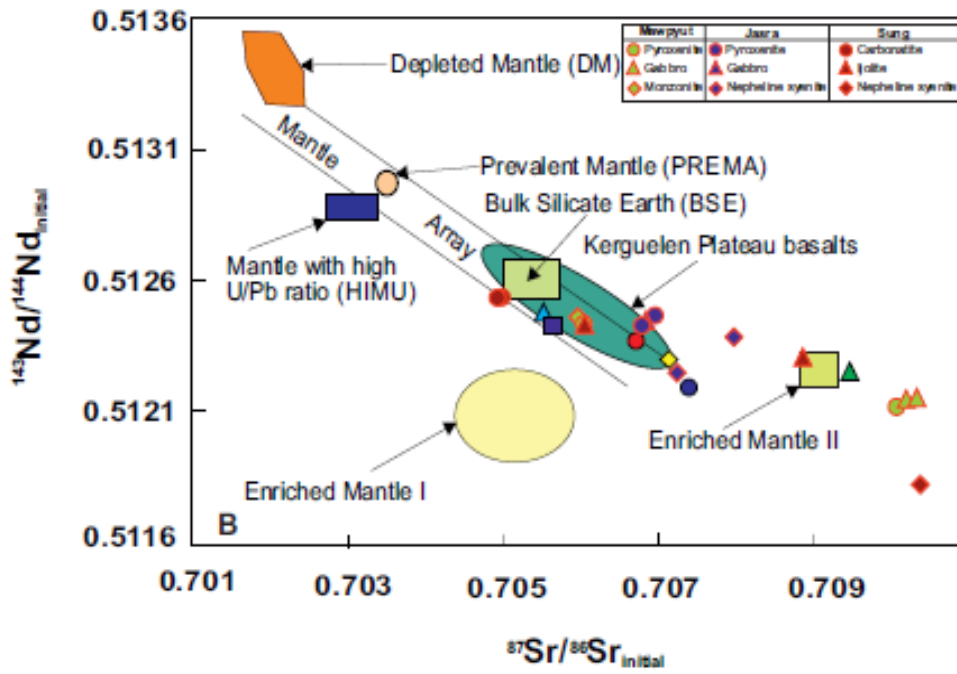
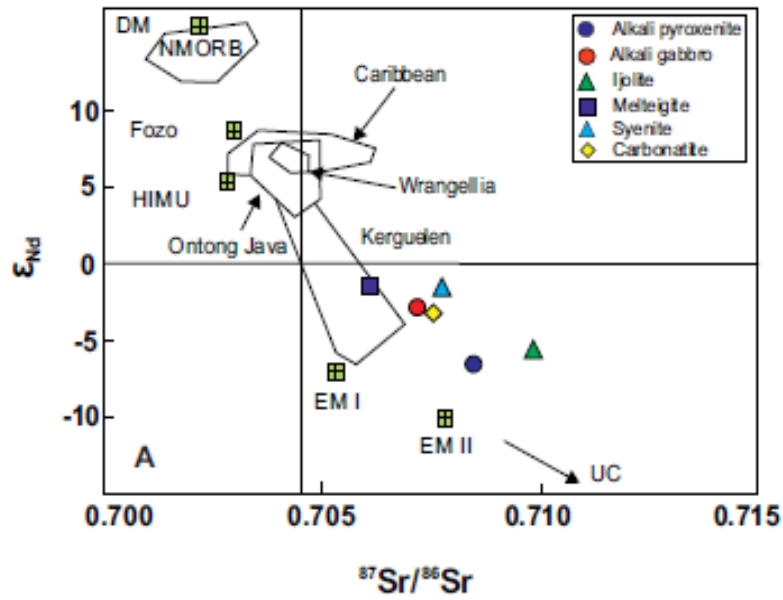


Fig.9

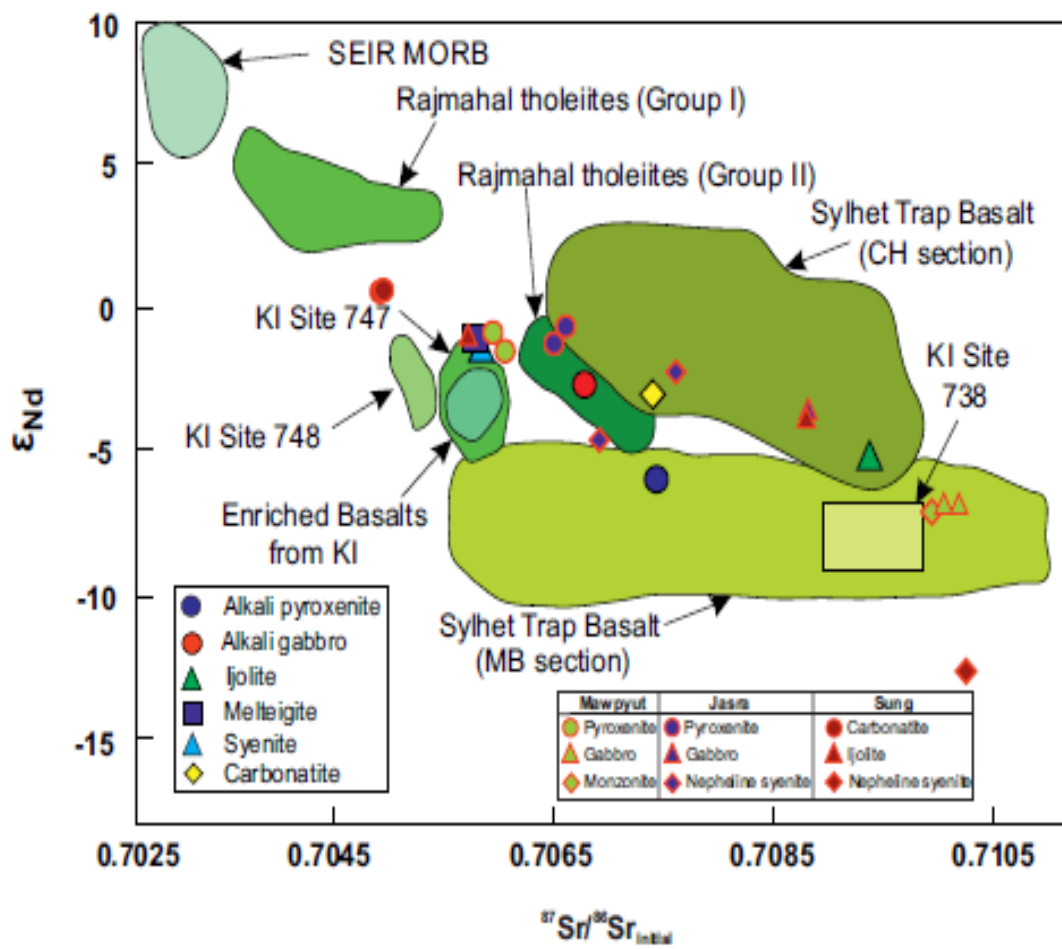


Fig.10

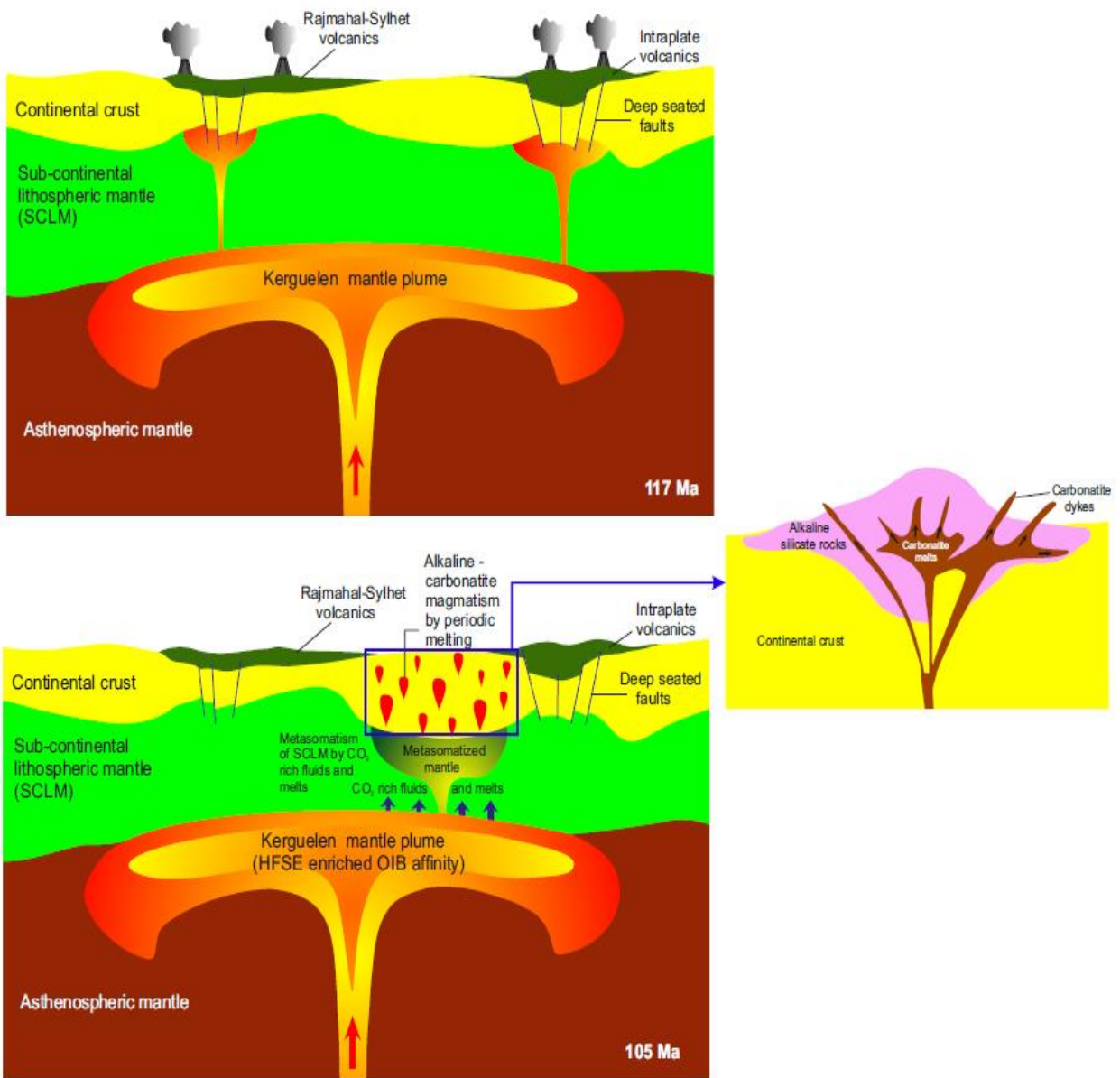


Fig.11

Table 1. Modal analyses of alkaline silicates and carbonatites of Samchampi-Samteran alkaline complex (SSAC)

Serial no.	1	2	3	4	5	6	7	8	9	10	11	12	13	14
Sample no.	SAJ 4A	SAJ 13	SAJ 14A	SAJ 15	SAJ 20	SAJ 29	SAJ 46	SAJ 47	SAJ58	SAJ 64	SAJ 3	SAJ 6	SAJ 7	SAJ10
K-feldspar	73.33	69	68.27	73.6	75.53	75.62	87.73	87.13	77.47	81.87	7.93	-	7.13	-
Plagioclase	5.8	3.2	2.2	-	-	-	4.27	5.88	-	-	-	-	-	-
Nepheline	-	-	-	-	-	-	-	-	-	-	55.27	48.25	50.87	11.8
Clinopyroxene	-	-	-	3.2	17.33	15.25	1.33	0.69	19.8	14.8	18.13	22.75	16.33	48
Amphibole	7.4	8.8	7.53	-	-	-	-	-	-	-	-	-	-	-
Biotite	-	2.66	3.53	-	-	-	0.87	0.6	-	1.33	11.07	9.78	16.73	11.2
Garnet	10.73	-	-	-	-	-	-	-	-	-	-	-	-	12
Carbonate	1.2	13	14	1	2.67	0.8	-	0.2	-	-	5	15.75	6.93	15.27
Ferruginous alteration	-	-	-	17.27	3.34	8.33	1.53	3.5	-	0.67	-	-	-	-
Sphene	0.87	1.67	2.14	-	1.13	-	-	0.27	2.6	1.2	0.4	-	1	0.53
Apatite	0.4	-	-	-	-	-	-	0.4	-	-	0.93	0.47	0.33	1.2
Opaque	0.27	1.67	2.33	4.93	-	-	4.27	1.33	0.13	0.13	1.27	3	0.68	-

Serial no. 1 to 10: syenites; 11 to 14: ijolite-melteigite

Table 1. Contd..

Serial no.	15	16	17	18	19	20	21	22	23	24	25	26	27	28
Sample no.	SAJ 15A	SAJ 16	SAJ 17	SAJ 18	SAJ 19	SAJ 23	SAJ 27	SAJ 33	SAJ 53	SAJ 11	SAJ 36	SAJ 51	SAJ 35	SAJ 4B
K-feldspar	-	-	-	-	-	1.6	-	-	1.93	-	-	3.73	27.93	20.38
Plagioclase	-	-	-	-	-	-	-	-	-	-	-	-	-	-
Nepheline	40.6	13.49	24	49.21	17.14	45.33	18.47	38.23	60.73	0.75	7.73	-	20.33	10.2
Clinopyroxene	50.33	53.67	35.6	46.93	61.57	34.4	81.53	51.86	32.27	96.4	91	90.47	33.67	64.16
Amphibole	-	-	-	-	-	-	-	-	-	-	-	-	-	-
Biotite	-	27.89	12.53	-	-	14.33	-	4.91	-	1.44	-	-	11.47	2.75
Garnet	-	-	13.27	-	-	-	-	-	-	-	-	-	-	-
Carbonate	6.67	1.63	8.67	-	17.79	1.07	-	5	1.33	1.3	-	3.8	1.4	-
Ferruginous alteration	-	-	-	-	-	-	-	-	-	-	-	-	-	-
Sphene	2.13	-	0.13	1.36	0.9	1.2	-	-	2.47	0.11	0.47	1.67	1.67	2.26
Apatite	0.27	0.67	0.93	2.5	0.5	1.6	-	-	0.47	-	0.4	0.33	0.8	0.25
Opaque	-	2.65	4.87	-	2.1	0.47	-	-	0.8	-	0.4	-	2.73	-

Serial no. 15 to 23: ijolite-melteigite; 24 to 28: alkali pyroxenites and alkali gabbros

Table 1. Contd...

Serial no.	29	30	31	32	33	34	35	36
Sample no.	SAJ 25	SAJ 26	SAJ 32	SAJ 30	SAJ 13A	SAJ 15A	SAJ 38	SAJ 39
K-feldspar	40.07	57.67	66.2	62.32	-	-	-	-
Plagioclase	-	-	-	-	-	-	-	-
Nepheline	37.33	14.87	25.93	12.75	-	-	-	-
Clinopyroxene	20.13	26.6	-	24.93	6.78	8.13	5.86	5.23
Amphibole	-	-	-	-	-	-	-	-
Biotite	2.27	0.66	-	-	8.36	7.26	14.57	15.23
Garnet	-	-	-	-	-	-	-	-
Carbonate	-	-	0.33	-	66.83	64.14	77.14	77.03
Ferruginous alteration	-	-	7.33	-	-	-	-	-
Sphene	-	-	0.21	-	-	-	-	-
Apatite	0.2	0.2	-	-	15.43	18.53	-	-
Opaque	-	-	-	-	2.6	1.94	2.43	2.51

Serial no. 29 to 32: nepheline syenites; 33 to 36: carbonatites

Table 2. Sr and Nd isotopic compositions in samples from Samchampi-Samteran alkaline complex (SSAC)

Rb-Sr Compositions

Sample	Rock type	Rb (ppm)	Sr (ppm)	$^{87}\text{Sr}/^{86}\text{Sr}$	2σ	$^{87}\text{Rb}/^{86}\text{Sr}$	$(^{87}\text{Sr}/^{86}\text{Sr})_{105}$	$\epsilon_{\text{Sr}}(105 \text{ Ma})$
SAJ11	Alkali pyroxenite	198	949	0.708506	0.000003	0.762706	0.707368	56.9
SAJ4B	Alkali gabbro	98.3	1536	0.707262	0.000004	0.372699	0.706706	39.2
SAJ17	Melteigite	46	993	0.706127	0.000003	0.324768	0.705642	23.1
SAJ7	Ijolite	184	3884	0.709906	0.000003	0.328666	0.709416	76.7
SAJ 4A	Syenite	295	604	0.707824	0.000003	1.516185	0.705562	47.2
SAJ13A	Carbonatite	9.0	2761	0.707594	0.000004	0.209172	0.707282	43.9

Sm-Nd Compositions

Sample	Rock type	Sm (ppm)	Nd (ppm)	$^{143}\text{Nd}/^{144}\text{Nd}$	2σ	$^{147}\text{Sm}/^{144}\text{Nd}$	$(^{143}\text{Nd}/^{144}\text{Nd})_{105}$	$\epsilon_{\text{Nd}}(105 \text{ Ma})$
SAJ11	Alkali pyroxenite	16.3	79.7	0.512312	0.000003	0.181717	0.512187	-6.37
SAJ4B	Alkali gabbro	10.4	67	0.512493	0.000003	0.155544	0.512386	-2.83
SAJ17	Melteigite	35.3	133	0.512573	0.000003	0.214122	0.512426	-1.27
SAJ7	Ijolite	18.5	109	0.512356	0.000003	0.163231	0.512244	-5.50
SAJ 4A	Syenite	5.9	35.6	0.512559	0.000002	0.160689	0.512449	-1.54
SAJ13A	Carbonatite	286	1505	0.512479	0.000004	0.174043	0.512359	-3.10

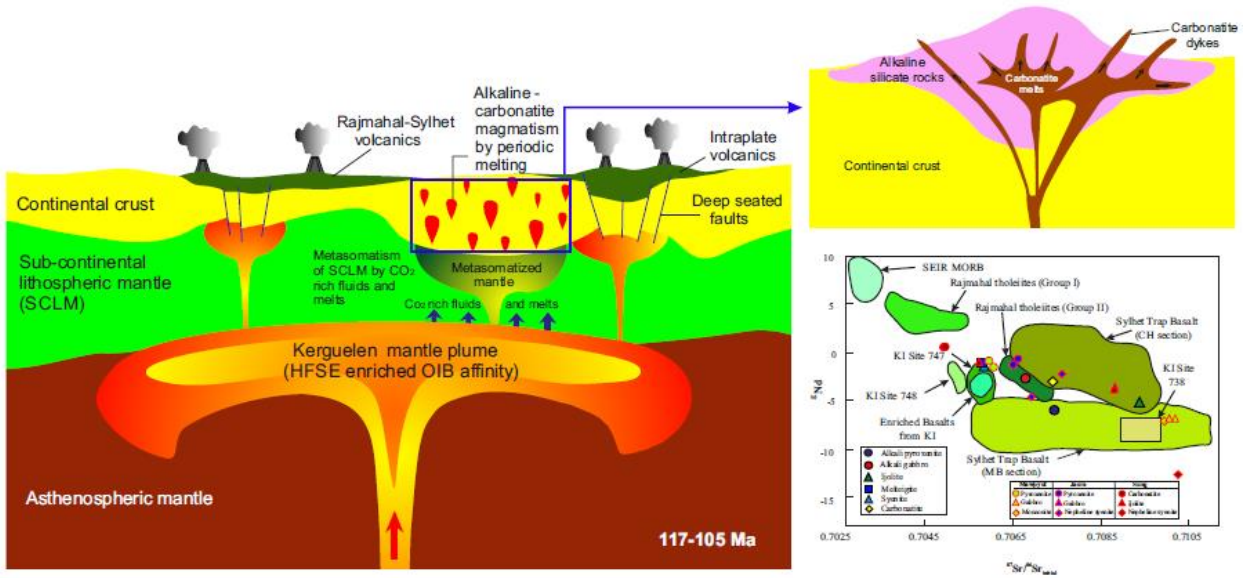
Initial Sr and Nd isotopic ratios along with epsilon values were calculated assuming an emplacement age of 105 Ma (after Heanman et al., 2002; Acharyya et al., 1986). Epsilon values are calculated using present-day ratios of $^{87}\text{Sr}/^{86}\text{Sr} = 0.7045$ (De Paolo, 1988) and $^{87}\text{Rb}/^{86}\text{Sr} = 0.0827$ (De Paolo, 1988) for Bulk Silicate Earth (BSE); $^{143}\text{Nd}/^{144}\text{Nd} = 0.512638$ (Goldstein et al., 1984) and $^{147}\text{Sm}/^{144}\text{Nd} = 0.1967$ (Jacobsen and Wasserburg, 1980) for Chondritic Uniform Reservoir (CHUR).

Table 3. A brief account of available geochemical features, isotopic and geochronological data for alkaline-carbonatite complexes of Shillong Plateau-Mikir Hills

Complex	Geochemical signatures	Isotopic composition	Source characteristics	Method and Age (in Ma)
Sung Valley	Incompatible trace element enrichment relative to primitive mantle, variable HFSE abundances, pronounced LREE/HREE fractionation	$^{87}\text{Sr}/^{86}\text{Sr}_{\text{initial}}$: 0.704830–0.710371; $^{143}\text{Nd}/^{144}\text{Nd}_{\text{initial}}$: 0.511845–0.512541; ϵ_{Sr} : +4.7 - +85.1; ϵ_{Nd} : -12.8–1.8 (Srivastava et al., 2005)	EM II and HIMU mixing producing FOZO signatures	1. Ar-Ar dating of pyroxenite and phlogopite from carbonatite: 107.2 ± 0.8 Ma; 2. Rb-Sr dating of carbonatite, pyroxenite, phlogopite from carbonatite: 106 ± 11 Ma; 3. U-Pb dating of perovskite from ijolite: 115.1 ± 5.1 Ma (Ray et al., 1999, 2000; Srivastava et al., 2005)
Jasra	LREE enriched patterns, negligible to positive Nb-Ta anomalies, OIB-type chemistry precluding crustal contamination	$^{87}\text{Sr}/^{86}\text{Sr}_{\text{initial}}$: 0.706523 - 0.708891; $^{143}\text{Nd}/^{144}\text{Nd}_{\text{initial}}$: 0.512258 - 0.512464; ϵ_{Sr} : 30.5–64.1; ϵ_{Nd} : -0.76–4.78 (Srivastava and Sinha, 2007)	Mixing of EM and HIMU showing isotopic signature resembling FOZO	U-Pb dating of zircon and baddeleyite from differentiated gabbro: 105.2 ± 0.5 Ma (Heaman et al., 2002)
Samchampi-Santeran	Pronounced LILE enrichment, Strong LREE/HREE fractionation, positive Nb-Ta and negative K, Th, Sr anomalies	$^{87}\text{Sr}/^{86}\text{Sr}_{\text{initial}}$: 0.705562–0.709416; $^{143}\text{Nd}/^{144}\text{Nd}_{\text{initial}}$: 0.512187–0.512449; ϵ_{Sr} : 23.1 - 76.7; ϵ_{Nd} : -6.37 to -1.27 (Present Study)	EMII	Fission track dating of apatite: ~105 (Acharya et al., 1986)
Mawpyut	Cumulate rocks show flat LREE and MREE patterns with moderate positive Eu anomaly; non-cumulate rocks show strongly fractionated REE patterns with no Eu anomaly	$^{87}\text{Sr}/^{86}\text{Sr}_{\text{initial}}$: 0.705954–0.710277; $^{143}\text{Nd}/^{144}\text{Nd}_{\text{initial}}$: 0.512137–0.512458; ϵ_{Sr} : 27.2 - 89.7; ϵ_{Nd} : -0.89 to -7.14 (Chaudhuri et al., 2014)	EMI/EMII/HIMU	No geochronological data available
Swangkre-Rongmil	LILE and HFSE enrichment relative to primitive mantle	Isotopic data not available till date		K-Ar dating of lamprophyre dyke: 107 ± 3 Ma (Srivastava and Sinha, 2004)

Research Highlights:

- New whole rock geochemical and Sr-Nd isotope data from SSAC
- Carbonatites derived by direct melting of metasomatized mantle peridotite
- Sr-Nd isotope systematics point towards an enriched mantle source
- Sr-Nd isotope systematics infer genetic association of SSAC with Sylhet Traps and Kerguelen plume



Graphical abstract